# Supporting Information

Catalytic Alkyne and Diyne Metathesis with Mixed Fluoroalkoxy-Siloxy Molybdenum Alkylidyne Complexes

Manuel L. Zier,[a] Sophie Colombel-Rouen,[b] Henrike Ehrhorn,[a] Dirk Bockfeld,[a] Yann Trolez,[b] Marc Mauduit,[b] Matthias Tamm[a,*]

[a] Institut für Anorganische und Analytische Chemie, Technische Universität Braunschweig, Hagenring 30, 38106 Braunschweig, Germany, Fax: +49 (531) 391 5387; Tel: +49 (531) 391 5309; E-Mail: m.tamm@tu-bs.de

[b] Univ Rennes; Ecole Nationale Supérieure de Chimie de Rennes, CNRS, ISCR – UMR 6226, F-35000 Rennes, France

# Experimental Section

## General Experimental Considerations

Synthesis of the molecular precursors was carried out according to the literature using dry and oxygen free argon glovebox atmosphere (MBraun) or were prepared using high vacuum lines ($10^{-5}$ mbar). *n*-Pentane, *n*-hexane, THF, and toluene were purified using double MBraun SPS alumina columns and degassed by argon-bubbling for at least 15 min prior to use. Hexamethyldisoloxane (HMDSO) was dried over $CaH_2$ and refluxed for three days. The solvents were stored over molecular sieves 3–4 Å inside a glovebox. Benzene-$d_6$ was degassed by three consecutive freeze-pump-thaw cycles and stirred overnight with NaK-alloy. Dichloromethane-$d_2$ was distilled over $CaH_2$. 1-Phenyl-1-propyne was distilled over $CaH_2$ and then filtered through alumina that had been activated under high vacuum at 500 °C ($Al_2O_{3\text{-}500}$). 1-Phenyl-1-propyne was used immediately after being filtered over $Al_2O_{3\text{-}500}$. Complexes and catalysts [MesC≡MoBr$_3$(dme)][1], [MesC≡Mo{OC(CF$_3$)$_n$Me$_{3-n}$}$_3$ (**MoF0**, $n = 0$, **MoF3**, $n = 1$, and **MoF9**, $n = 3$)[2] and KOSi(O*t*Bu)$_3$[3] were synthesized according to literature methods. The silicate HOSi(O*t*Bu)$_2$(OMes)[4] was synthesized according to the literature. Celite was dried over night at 130 °C and then under vacuum for 5 h, before storing it in the glovebox. The powdered molecular sieves Molecular sieves 4 Å (CAS: 70955-01-0; Ref. No. 11424553 Alfa Aesar™) and 5 Å (CAS : 69912-79-4; Ref. No. 10296980 Acros Organics™) were heated in oven (~ 400 °C for 24 hours) then vacuum ($10^{-2}$ mmbar for 24h) was applied prior to introduction into the glove box.

## Analytical Methods

Solution $^1$H, $^{13}$C and $^{19}$F NMR Spectra were obtained on *Bruker AV II-300* (300 MHz), *Bruker AV II-400* (400 MHz) or *Bruker AV II-600* (600 MHz) instruments at room temperature. Variable temperature and 2D NMR experiments were carried out on *Bruker AV II-400* (400 MHz) or *Bruker AV II-600* (600 MHz). Low temperature measurements where calibrated with $CH_3OH$ in $CD_3OD$, high temperature measurements where calibrated with $HOCH_2CH_2OH$ in DMSO-$d_6$. The $^1$H and $^{13}$C chemical shifts are referenced to the solvent peak, and the $^{19}$F chemical shifts are referenced relative to virtual internal $CFCl_3$. All $^{13}$C and $^{19}$F NMR Spectra were measured $^1$H decoupled. Spin multiplicity is designated by: s, singlet; d, doublet; t, triplet; q, quartet; sept, septet; m, multiplet. The number of protons (n) for a given resonance is indicated by nH. Chemical shifts ($\delta$) are reported in parts per million (ppm) and coupling constants ($J$) are reported in Hz. The NMR data were interpreted in first order spectra. Gas chromatography (GC) was performed on a *HP 5890 Series II* using DB5-HT column ($l$ = 30 m, $d$ = 0.25 mm) with FID detection (310 °C). The sample (1 µL) was injected at 250 °C with a split(splitless ratio of 1:10 and heated in the column from 50 to 300 °C with a heating rate of 10 °C min$^{-1}$. For calibration, *n*-decane was used as an internal standard. GCMS was performed on a *GC-2010 SHIMADZU* coupled directly with a *QP2010SE* mass spectrometer operating in positive EI mode (70 eV, 60 – 700 m/z) with the following conditions: injection temperature 50 °C for 3 min, heating rate 12 °C min$^{-1}$, end temperature 300 °C for 38 min; column type: ZB-5MS GUARDIAN ($l$ = 30 m, $d$ = 0.25 mm); He carrier gas (1.5 mL min$^{-1}$). Elemental analyses were performed by using a *Vario Micro Cube* with WLD and IR detectors.

## Experimental Procedures

### Synthesis of [MesC≡Mo{OC(CF$_3$)$_3$}$_2${OSi(O*t*Bu)$_3$}] (MoSiF9)

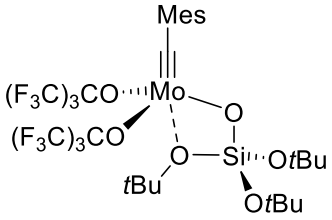


To a solution of KOSi(O*t*Bu)$_3$ (56.8 mg, 0.19 mmol) in toluene (4 mL) was added [MesC≡Mo{OC(CF$_3$)$_3$}$_3$] (**MoF9**) (174.9 mg, 0.19 mmol), and the reaction mixture was stirred for 16 h at 40 °C. After evaporation of the solvent, the residue was extracted with *n*-pentane (2 mL); the solution was filtered over Celite and stored at −38 °C. The product was obtained as yellow crystals (169.9 mg, 0.18 mmol, 93%).

**$^1$H NMR** (300 MHz, C$_6$D$_6$, 298 K): $\delta$ = 6.56–6.47 (m, 2H, $H_{Ar}$), 2.78 (s, 6H, *o*-C$H_3$), 2.01 (s, 3H, *p*-C$H_3$), 1.33 (s, 27H, OSi(OC(C$H_3$)$_3$)$_3$) ppm. **$^{13}$C{$^1$H} NMR** (75.5 MHz, C$_6$D$_6$, 298 K): $\delta$ = 320.9 (s, Mo≡*C*), 143.3 (s, *o*-$C_{Ar}$), 142.8 (s, *i*-$C_{Ar}$), 140.5 (s, *p*-$C_{Ar}$), 128.1 (s, $CH_{Ar}$), 121.5 (q, $^1J_{C,F}$ = 292 Hz, OC(*C*F$_3$)$_3$), 85.3 (sept, $^2J_{C,F}$ = 30 Hz, OC(CF$_3$)$_3$), 75.3 (s, OSi(O*C*(CH$_3$)$_3$)$_3$), 31.2 (s, OSi(OC(*C*H$_3$)$_3$)$_3$), 21.0 (s, *p*-CH$_3$), 20.4 (s, *o*-CH$_3$) ppm. **$^{19}$F{$^1$H} NMR** (376.1 MHz, C$_6$D$_6$, 298 K): $\delta$ = −72.9 (s, C*F*$_3$) ppm. **Elemental analysis** (%) calc. for C$_{30}$H$_{38}$F$_{18}$MoO$_6$Si: C 37.51, H 3.99; Found: C 37.83, H 4.04.

### Synthesis of KOSi(O*t*Bu)$_2$(OMes)

HOSi(O*t*Bu)$_2$(OMes) (1.2 mmol, 0.4 g) was dissolved in diethyl ether (5 mL), and KH (1.2 mmol, 48.12 mg) was added in small portions. After stirring the reaction mixture for 4h at rt, the solvent was evaporated, and the product was isolated as a white solid (0.39 g, 1.09 mmol, 92%).

**$^1$H NMR** (300 MHz, C$_6$D$_6$, 298K): $\delta$ = 6.77 (s, 2H, *m*-C*H*), 2.49 (s, 6H, *m*-C$H_3$), 2.09 (s, 3H, *p*-C$H_3$), 1.44 (s, 18H, OC(C$H_3$)$_3$) ppm. **$^{13}$C{$^1$H} NMR** (126 MHz, C$_6$D$_6$, 298K): $\delta$ = 152.2 (s, *ipso-C*), 129.7 (s, *o-C*), 129.6 (s, *p-C*), 129.2 (s, *m-C*), 71.3 (s, O*C*(CH$_3$)$_3$), 32.3 (s, OC(*C*H$_3$)$_3$), 20.5 (s, *p*-CH$_3$), 19.4 (s, *m*-CH$_3$) ppm. **$^{29}$Si{$^1$H} NMR** (99 MHz, C$_6$D$_6$, 298K): $\delta$ = −91.0 (s, *Si*) ppm. **Elemental analysis** (%) calc. for C$_{17}$H$_{29}$KO$_4$Si: C 56.00, H 8.02; Found: C 56.38, H 8.19.

### Synthesis of [MesC≡Mo{OC(CF$_3$)$_3$}$_2${OSi(OMes)(O*t*Bu)$_2$}] (MoSi*F9)

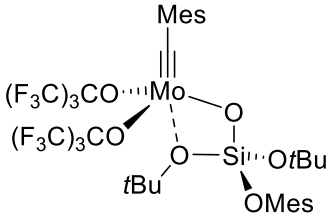


To a solution of [MesC≡Mo{OC(CF$_3$)$_3$}$_3$] (**MoF9**) (100 mg, 0.011 mmol) in toluene (2 mL) was added KOSi(O*t*Bu)$_2$(OMes) (39.1 mg, 0.11 mmol) and stirred over night at room temperature. After evaporation of the solvent, the crude product was extracted with HMDSO and filtered over Celite. Recrystallization at −38 °C afforded the product as yellow crystals (62.8 mg, 0.06 mmol, 56%).

**$^1$H NMR** (500 MHz, C$_6$D$_6$, 298 K): $\delta$ = 6.72 (m, 2H, SiOMesH$_{Ar}$), 6.47–6.45 (m, 2H, MoCMesH$_{Ar}$), 2.70 (s, 6H, MoCMes (*o*-CH$_3$)), 2.40 (s, 6H, SiOMes (*o*-CH$_3$)), 2.10 (s, 3H, MoCMes (*p*-CH$_3$)), 1.95 (s, 3H, SiOMes (*p*-CH$_3$)), 1.26 (s, 18H, OSi(OC(C$H_3$)$_3$) ppm. **$^{13}$C{$^1$H} NMR** (126 MHz, C$_6$D$_6$, 298 K): $\delta$ = 323.5 (s, MoC), 149.0 (s, SiOMes *i*-$C_{Ar}$), 143.2 (s, *i*-$C_{Ar}$), 142.7 (s, *o*-$C_{Ar}$), 141.1 (s, *p*-$C_{Ar}$), 131.6 (s, SiOMes *o*-$C_{Ar}$), 129.7 (s, SiOMes *m*-$C_{Ar}$), 128.4 (s, SiOMes *p*-$C_{Ar}$), 127.9 (s, *m*-$C_{Ar}$, 121.4 (q, $^1J_{C,F}$ = 292 Hz, *C*F$_3$), 85.3 (sept, $^2J_{C,F}$ = 30 Hz, *C*CF$_3$), 75.7 (s, OCCH$_3$), 30.9 (s, OCCH$_3$), 21.1 (s, SiOMes *p*-CH$_3$), 20.6 (s, MoCMes *p*-CH$_3$), 20.0 (s, MoCMes *o*-CH$_3$), 17.9 (s, SiOMes *o*-CH$_3$) ppm. **$^{19}$F{$^1$H} NMR** (377 MHz, C$_6$D$_6$, 298 K): $\delta$ = −73.1 (s, C*F*$_3$) ppm. **$^{29}$Si{$^1$H} NMR** (99 MHz, C$_6$D$_6$,

298 K): $\delta$ = −93.0 (s, *Si*) ppm. **Elemental analysis** (%) calc. for $C_{35}H_{40}F_{18}MoO_6Si$: C 41.10, H 3.94; Found: C 40.72, H 3.71.

### Synthesis of [(Et$_3$C$_3$)Mo{OC(CF$_3$)$_3$}$_2${OSi(O*t*Bu)$_3$}] (MoSiF9-MCBD)

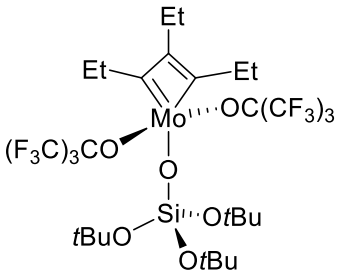


To a precooled solution of [MesC≡Mo{OC(CF$_3$)$_3$}$_2$ {OSi(O*t*Bu)$_3$}] (**MoSiF9**) (10 mg, 0.01 mmol) in *n*-pentane (0.1 mL) was added 3-hexyne (12 µL, 8.55 mg, 0.1 mmol). The mixture was immediately stored in the freezer at −38 °C to slowly grow the product as violet crystals, which decompose above −38 °C.

**$^1$H NMR** (400 MHz, $CD_2Cl_2$, 233.55 K): $\delta$ = 1.40 (s, 27H, OSi(OC(C*H*$_3$)$_3$)$_3$), 1.43 (t, 3H, $^3J_{H,H}$ = 8 Hz, β-C*H*$_3$), 1.71 (t, 6H, $^3J_{H,H}$ = 7 Hz, α-C*H*$_2$), 3.63 (q, $^3J_{H,H}$ = 7 Hz, 4H, α−C*H*$_2$), 3.81 (q, $^3J_{H,H}$ = 8 Hz, 2H, β-C*H*$_2$) ppm. **$^{13}$C{$^1$H} NMR** (101 MHz, $CD_2Cl_2$, 233.55 K): $\delta$ = 265.5 (s, C$_q$, α-*C*), 152.3 (s, C$_q$, β-C), 121.0 (q, $^1J_{C,F}$ = 295 Hz, *C*F$_3$), 82.8–81.3 (m, C$_q$, *C*(CF$_3$)$_3$), 73.2 (s, C$_q$, *C*(CH$_3$)$_3$), 33.5 (s, α-*C*H$_2$), 31.3 (s, C(*C*H$_3$)$_3$), 29.0 (s, β-*C*H$_2$), 12.7 (s, α-*C*H$_3$), 12.3 (s, β-*C*H$_3$) ppm. **$^{19}$F{$^1$H} NMR** (377 MHz, $CD_2Cl_2$, 233.55 K): $\delta$ = −72.6 (s, C*F*$_3$) ppm.

### Synthesis of [(Et$_3$C$_3$)Mo{OC(CF$_3$)$_3$}$_2${OSi(OMes)(O*t*Bu)$_2$}] (MoSi*F9-MCBD)

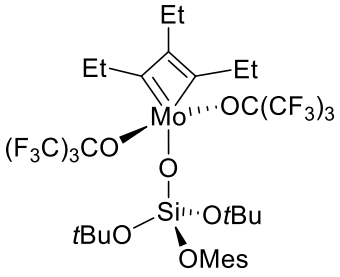


3-Hexyne (12 µL, 8.55 mg, 0.1 mmol) was added to a solution of [MesC≡Mo{OC(CF$_3$)$_3$}$_2${OSi(OMes)(O*t*Bu)$_2$}] (**MoSi*F9**) (10 mg, 0.01 mmol) in *n*-pentane (0.1 mL). The mixture was immediately stored in the freezer at −38 °C to slowly grow the product as violet crystals.

**$^1$H NMR** (500 MHz, Toluene-$d_8$, 298.15 K): $\delta$ = 6.80 (d, $^4J_{H,H}$ = 1 Hz, 2H, *H*$_{Ar}$), 3.15 (q, $^3J_{H,H}$ = 7 Hz, 4H, CαC*H*$_2$), 3.05 (q, $^3J_{H,H}$ = 8 Hz, 2H, CβC*H*$_2$), 2.58 (s, 6H, *o*-C*H*$_3$), 2.16 (s, 3H, *p*-C*H*$_3$), 1.57 (t, $^3J_{H,H}$ = 7 Hz, 6H, CαCH$_2$C*H*$_3$), 1.39 (s, 18H, OC(C*H*$_3$)$_3$), 0.91 (t, $^3J_{H,H}$ = 8 Hz, 3H) ppm. **$^{13}$C{$^1$H} NMR** (126 MHz, toluene-$d_8$, 298 K): $\delta$ = 265.1 (s, Cα), 151.1 (s, Cβ), 150.4 (s, SiOC$_q$), 130.3 (s, SiOCCCHC), 129.4 (s, SiOCCCH), 128.6 (s, SiOC*C*), 121.9 (q, $^1J_{C,F}$ = 295 Hz), 82.8 (m, $^2J_{C,F}$ = 29 Hz, *C*(CF$_3$)$_3$), 74.1 (s, SiO*C*(CH$_3$)$_3$), 33.0 (s, CαCH$_2$), 31.4 (s, SiOC(*C*H$_3$)$_3$), 28.1 (s, CαCH$_2$), 20.8 (s, *p*-CH$_3$), 18.3 (s, *o*-CH$_3$), 12.7 (s, CαCH$_2$CH$_3$), 12.4 (s, CβCH$_2$CH$_3$) ppm. **$^{19}$F{$^1$H} NMR** (471 MHz, toluene-$d_8$, 298.15 K): $\delta$ = −72.6 (s, C*F*$_3$) ppm. **$^{29}$Si{$^1$H} NMR** (99 MHz, toluene-$d_8$, 298 K): $\delta$ = −105.8 (s, *Si*) ppm.

### Reaction towards [MesC≡Mo{O*t*Bu}$_2${OSi(O*t*Bu)$_3$}] (MoSiF0)

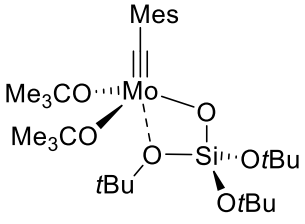


To a solution of KOSi(O*t*Bu)$_3$ (29.5 mg, 0.10 mmol) in toluene (2 mL) was added [MesC≡Mo{O*t*Bu}$_3$] (**MoF0**) (43.6 mg, 0.10 mmol), and the reaction mixture was stirred four hours at 40 °C. After evaporation of the solvent the residue was extracted with *n*-pentane (2 mL), filtered over Celite and stored at −38 °C. The product could only be isolated as mixture with the starting material and the corresponding bis- and tris(siloxide) complexes.

**$^1$H NMR** (300 MHz, $C_6D_6$, 298 K): $\delta$ = 6.70 (m, 2H, $H_{Ar}$), 2.89 (s, 6H, *o*-C$H_3$), 2.10 (s, 3H, *p*-C$H_3$), 1.53 (s, 18H, OC(C$H_3$)$_3$), 1.48 (s, 27H, OSi(OC(C$H_3$)$_3$)$_3$) ppm.

**Reaction towards [MesC≡Mo{OC(CF$_3$)Me$_2$}$_2${OSi(O*t*Bu)$_3$}] (MoSiF3)**

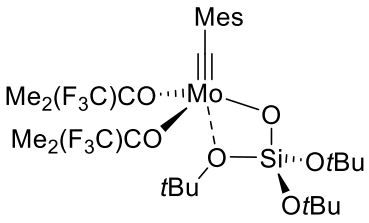


To a solution of KOSi(O*t*Bu)$_3$ (37.8 mg, 0.12 mmol) in toluene (2 mL) was added [MesC≡Mo{OC(CF$_3$)Me$_2$}$_3$] (**MoF3**) (76.1 mg, 0.12 mmol) and the reaction mixture was stirred four hours at 40 °C. After filtration over Celite and washing with toluene (1 mL), the solvent was evaporated. The residue was extracted with *n*-pentane (2 mL), filtrated over Celite and stored at −38 °C. The product could only be isolated as mixture with the corresponding bis- and tris(siloxide) complexes.

**$^1$H NMR** (300 MHz, $C_6D_6$, 298 K): $\delta$ = 6.71 (m, 2H, $H_{Ar}$), 2.89 (s, 6H, *o*-C$H_3$), 2.10 (s, 3H, *p*-C$H_3$), 1.43 (s, 12H, OC(C$H_3$)$_2$CF$_3$), 1.37 (s, 27H, OSi(OC(C$H_3$)$_3$)$_3$) ppm.

# NMR Spectra

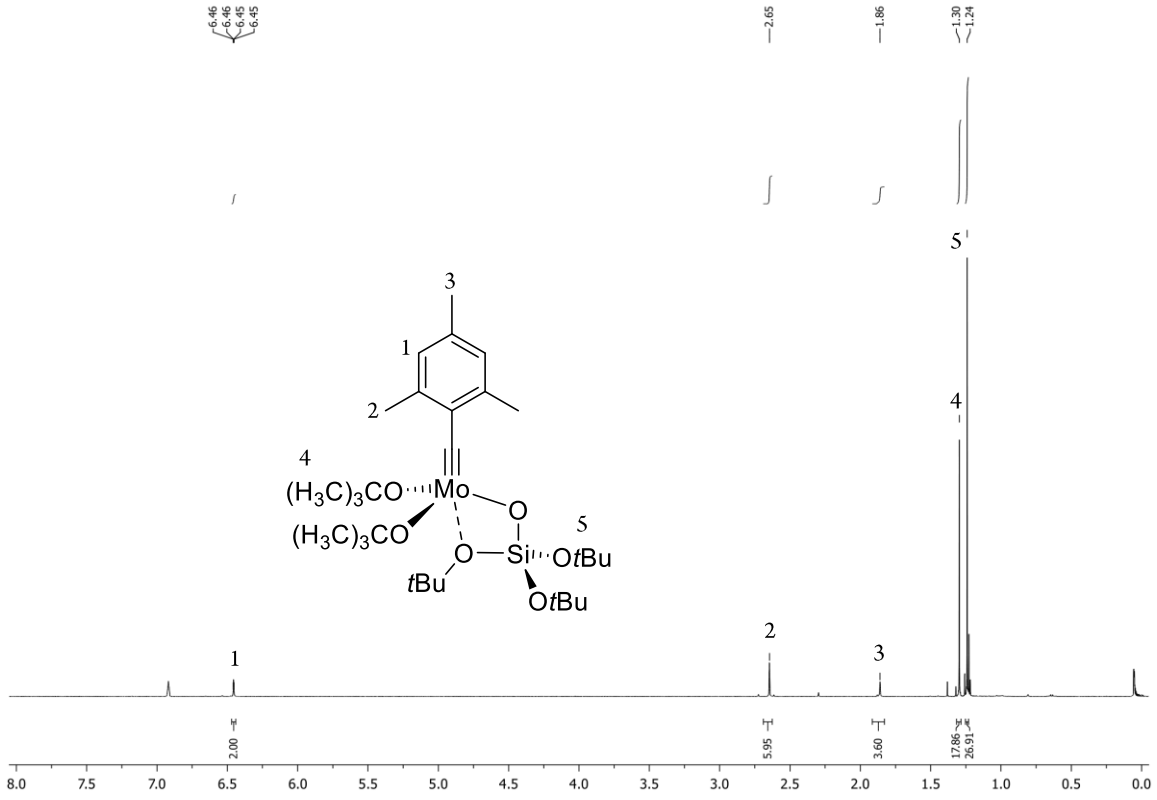


*Figure S1: Crude $^{1}H$ NMR spectrum of* ***MoSiF0*** in $C_6D_6$.

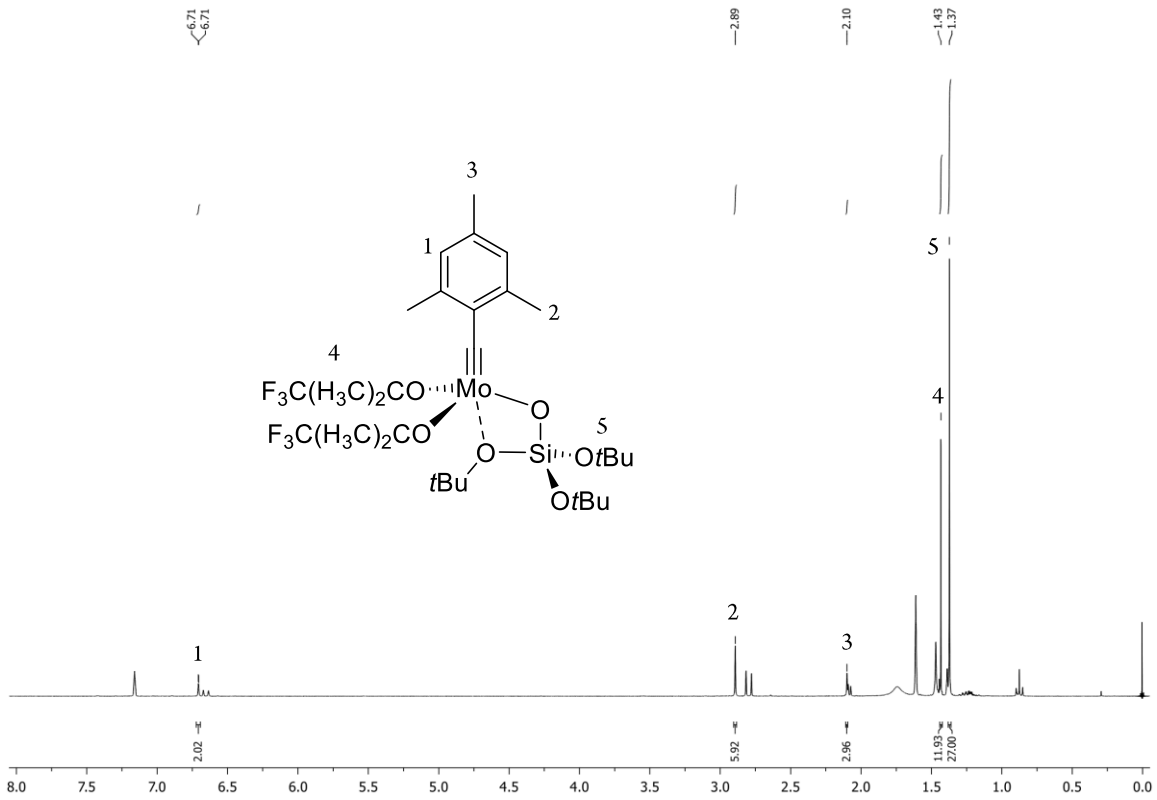


*Figure S2: Crude $^{1}H$ NMR spectrum of* ***MoSiF3*** in $C_6D_6$.

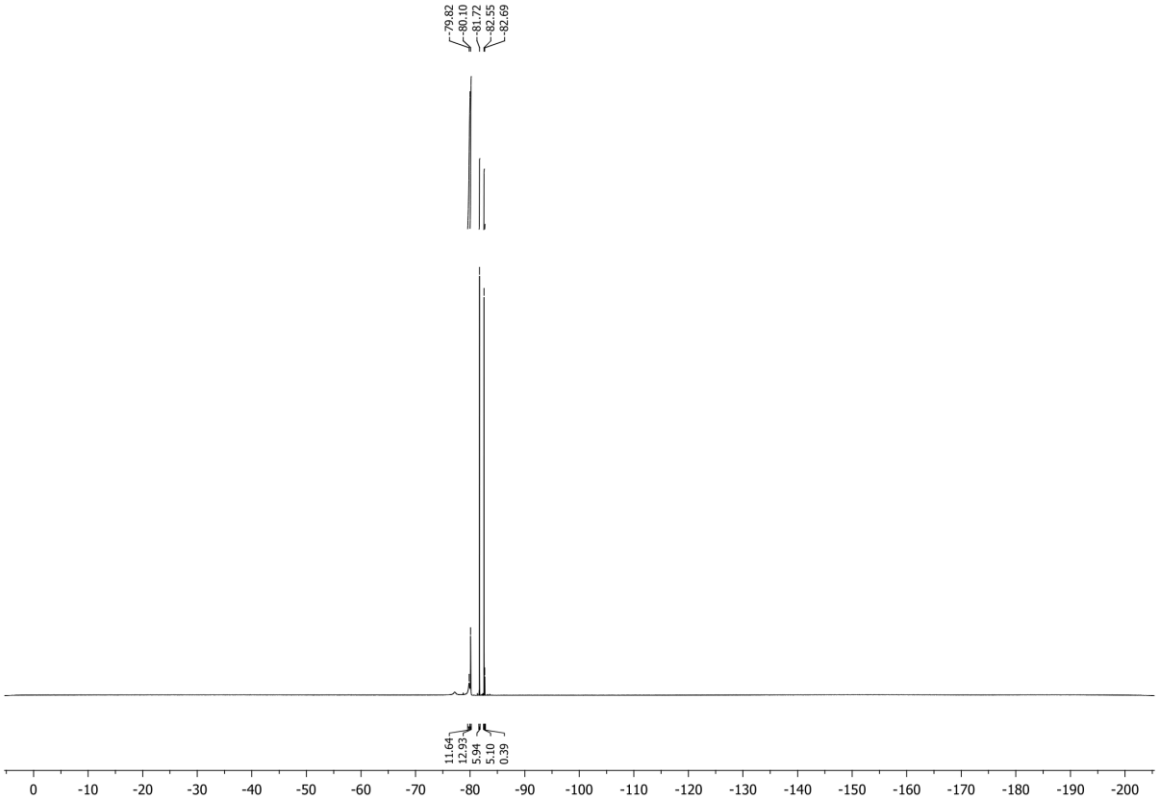


*Figure S3. Crude $^{19}F\{^{1}H\}$ NMR spectrum of* ***MoSiF3*** in $C_6D_6$.

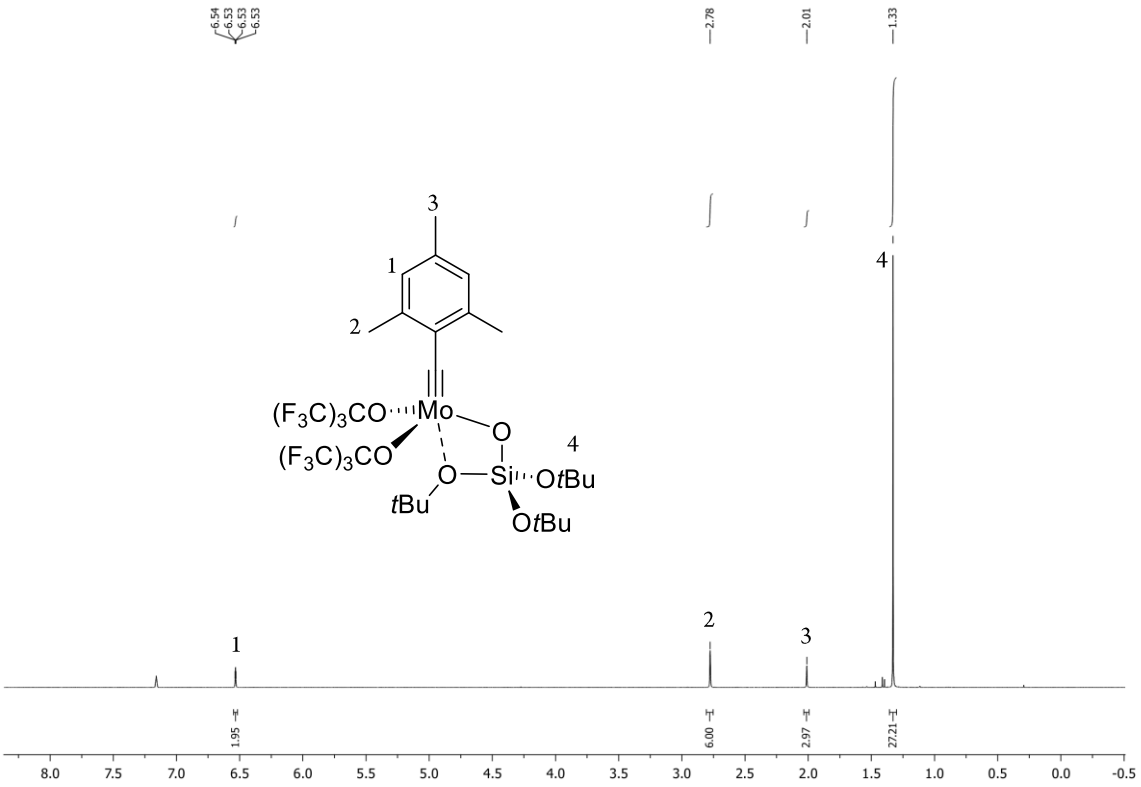


*Figure S4: $^{1}H$ NMR spectrum of* ***MoSiF9*** in $C_6D_6$.

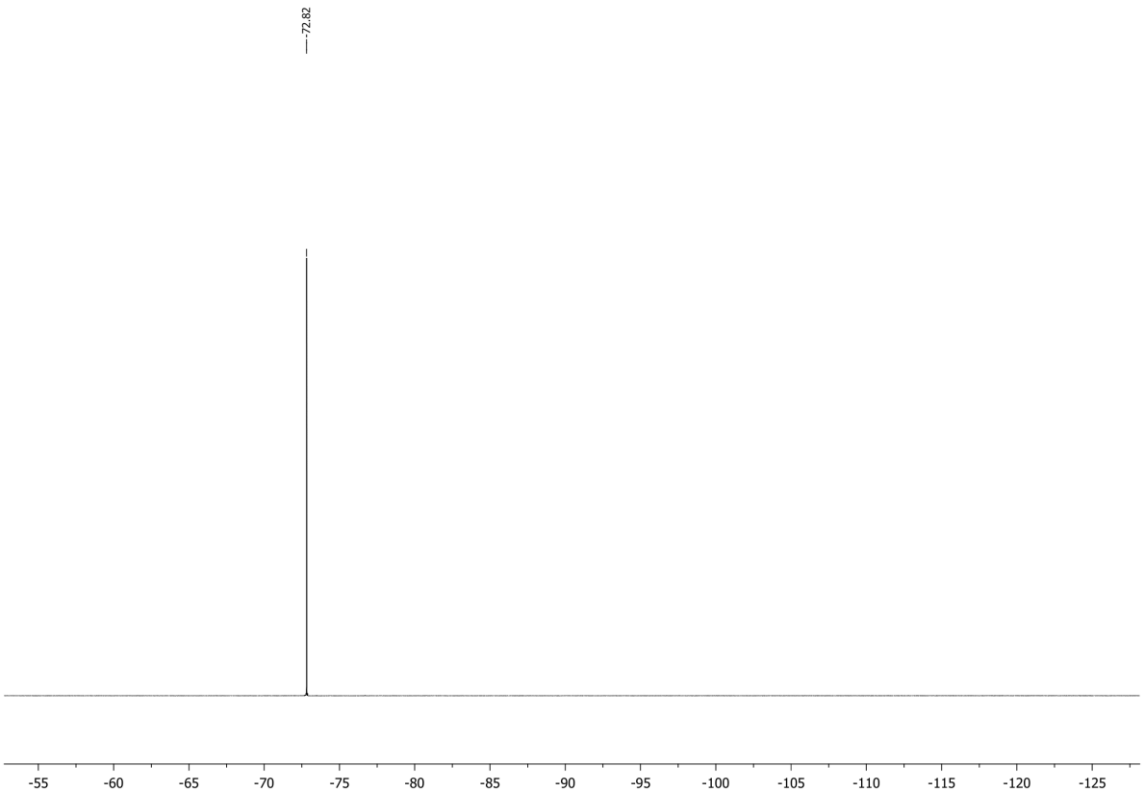


*Figure S5: $^{19}F\{H\}$ NMR spectrum of* ***MoSiF9*** in $C_6D_6$.

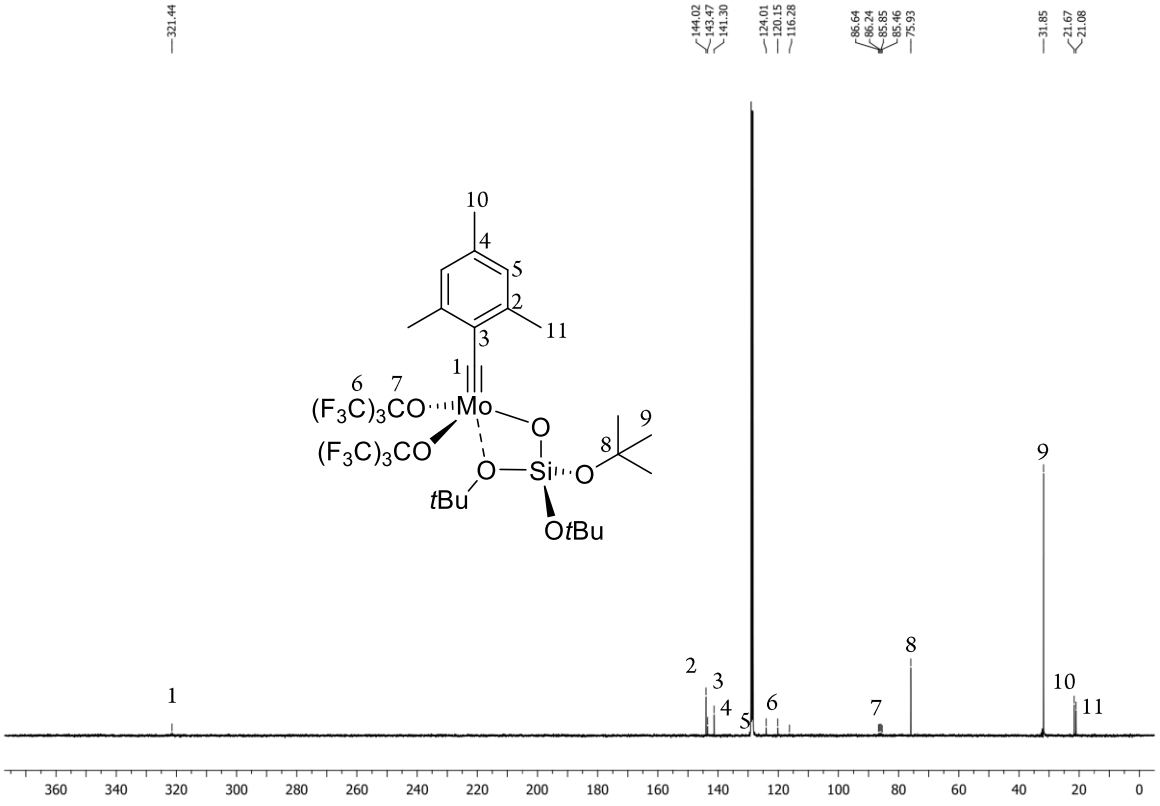


*Figure S6. $^{13}C\{H\}$ NMR spectrum of **MoSiF9** in $C_6D_6$.*

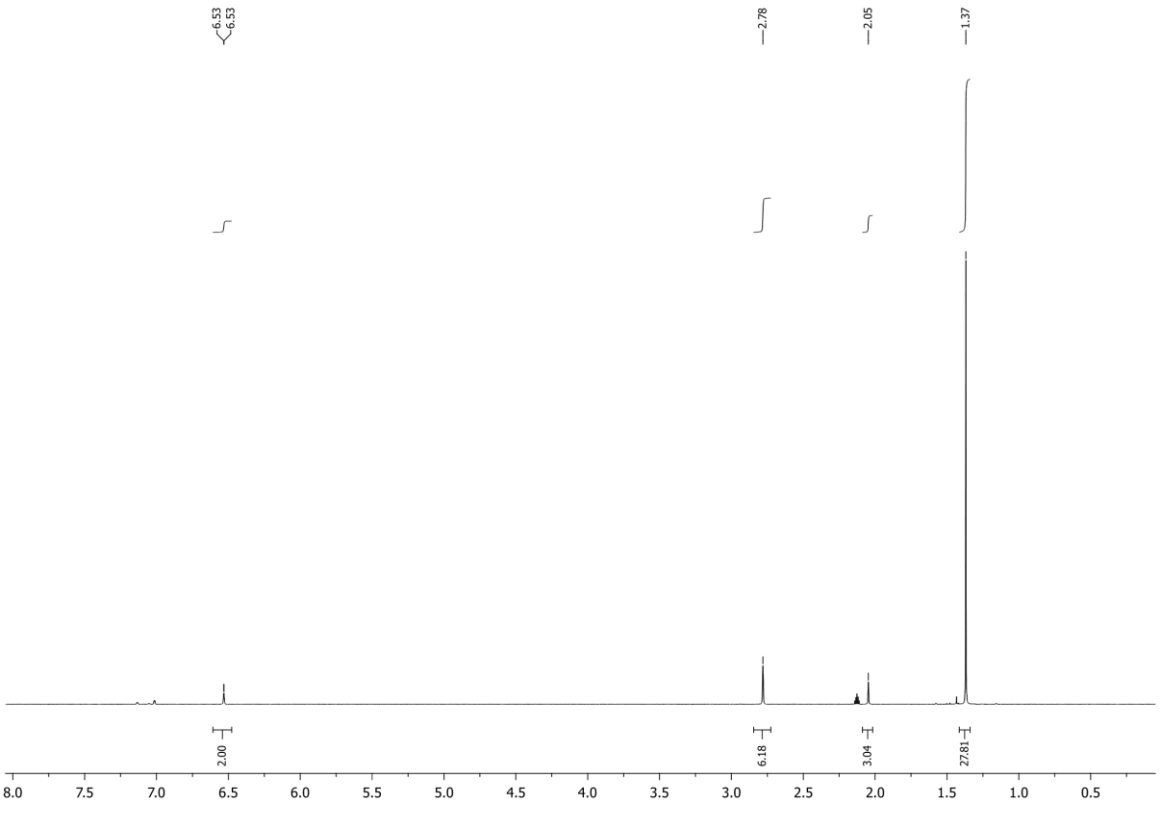


*Figure S7. $^{1}H$ NMR spectrum of **MoSiF9** in toluene-$d_8$.*

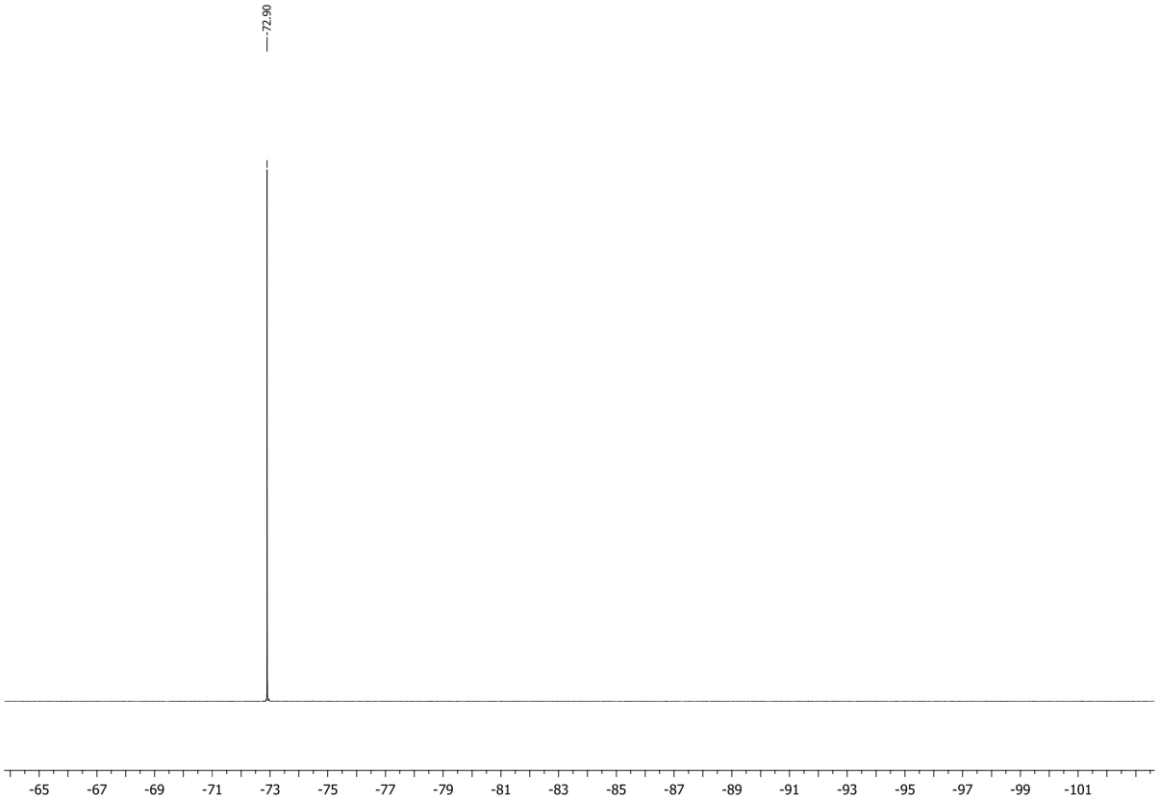


*Figure 8. $^{19}F\{^{1}H\}$ NMR spectrum of **MoSiF9** in toluene-$d_8$.*

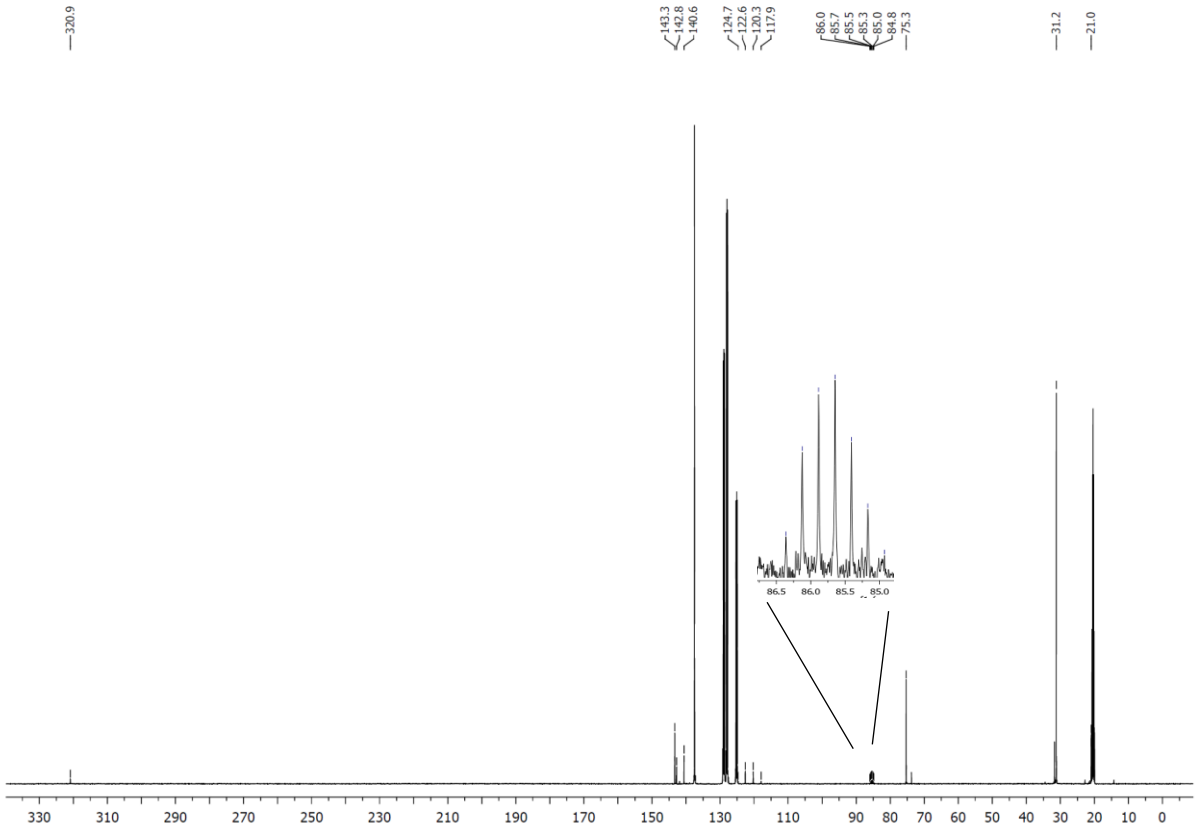


*Figure S9: $^{13}C\{H\}$ NMR spectrum of **MoSiF9** in toluene-d8.*

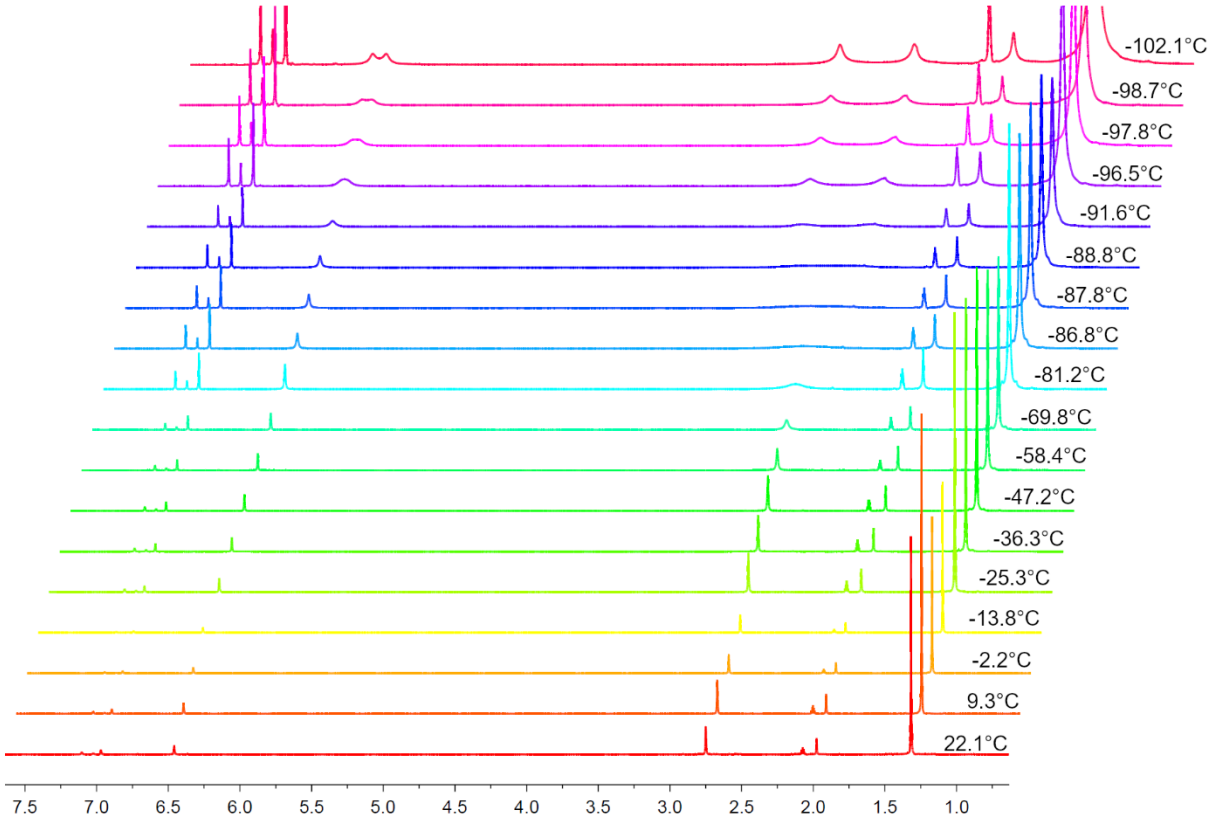


*Figure S10: $^{1}H$ variable temperature NMR spectrum of **MoSiF9** in toluene-d8.*

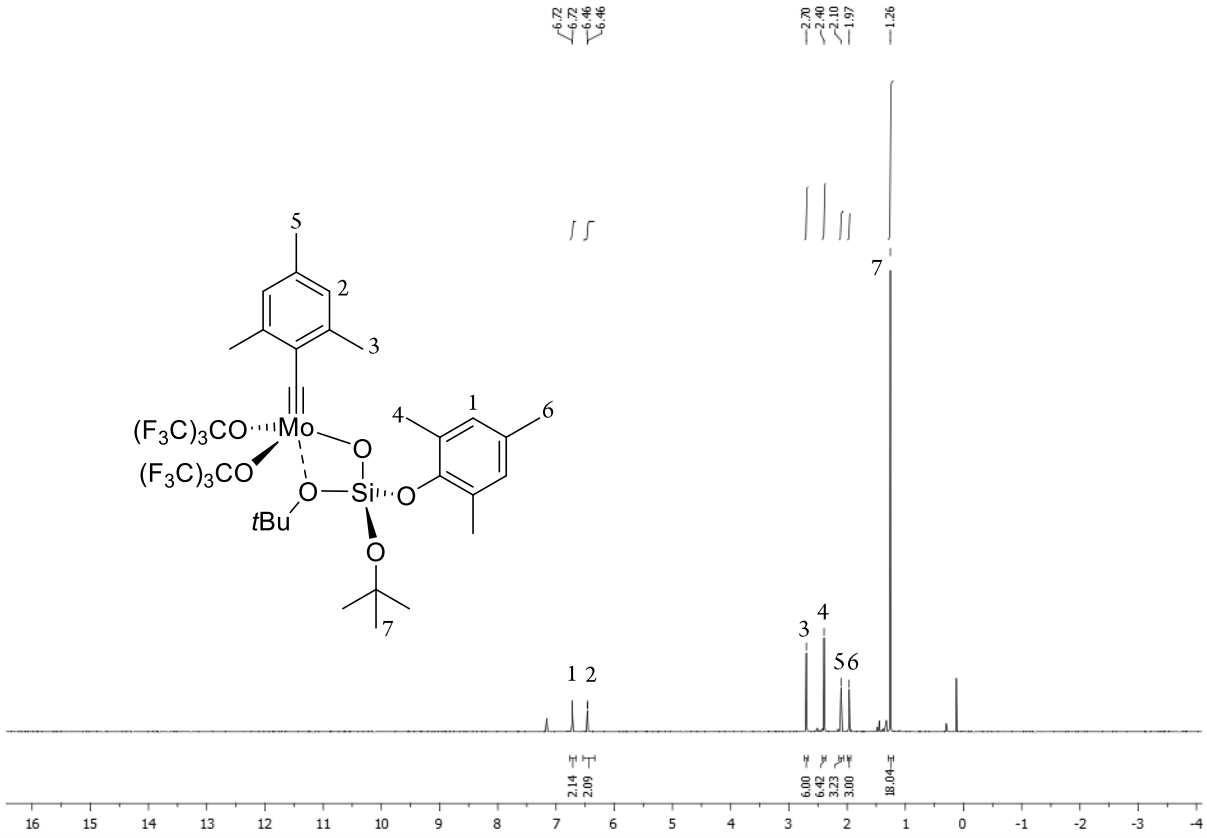


*Figure S11. $^{1}H$ NMR spectrum of **MoSi*F9** in $C_6D_6$.*

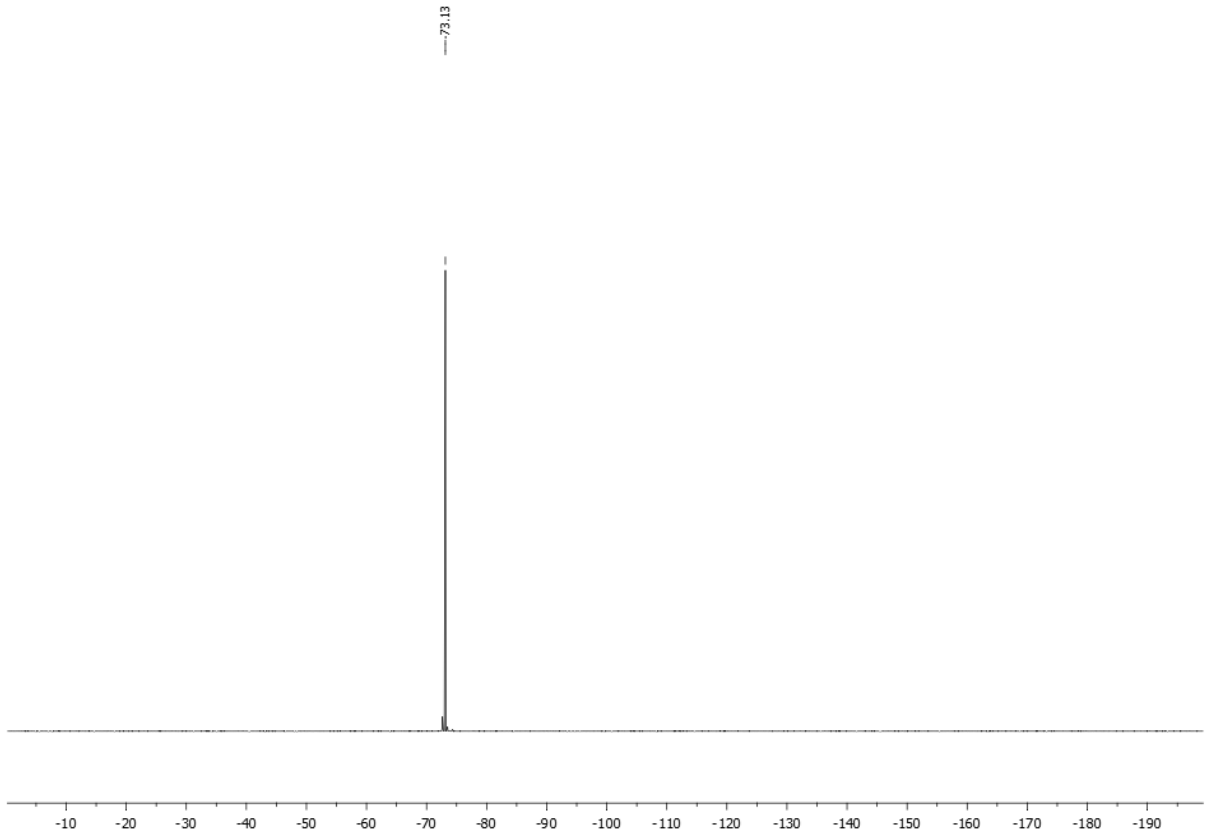


*Figure S12.* $^{19}F\{^{1}H\}$ *NMR spectrum of* ***MoSi*F9*** *in* $C_6D_6$.

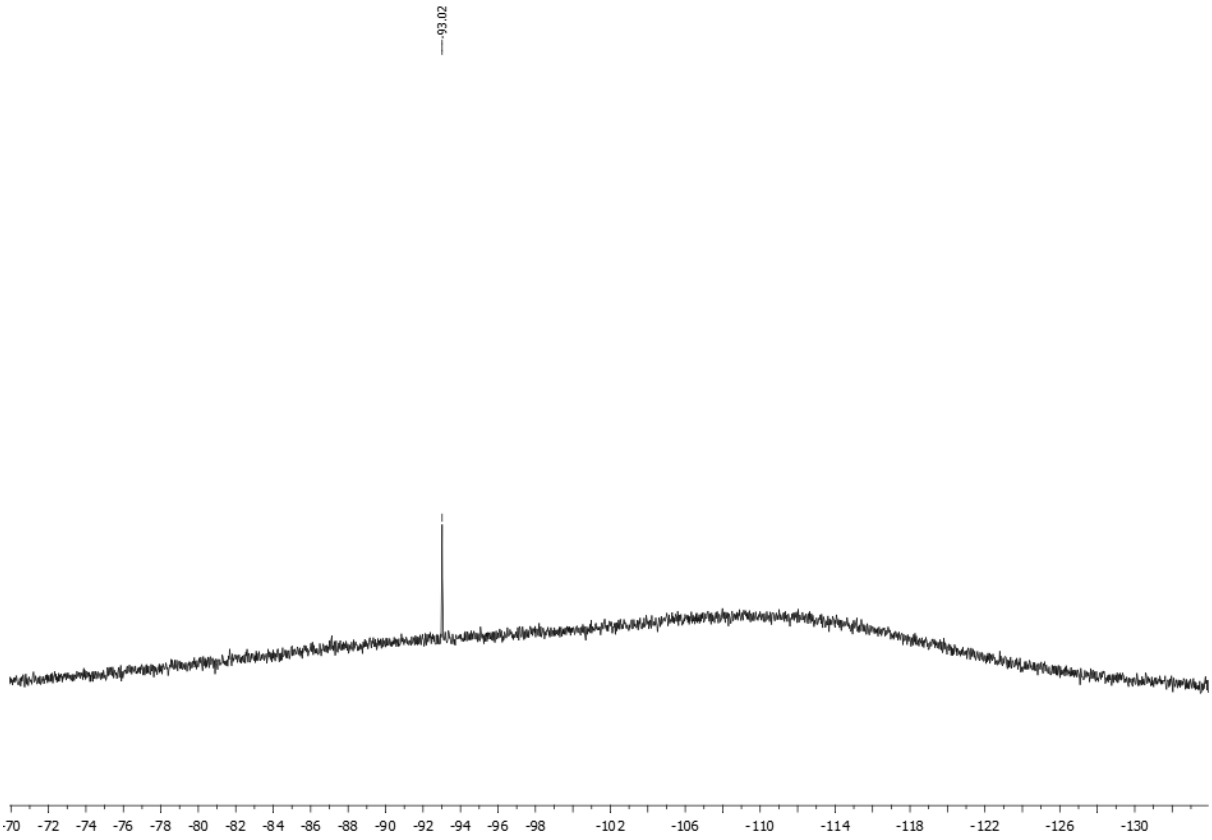


*Figure S13.* $^{29}Si$ *NMR spectrum of* ***MoSi*F9*** *in* $C_6D_6$.

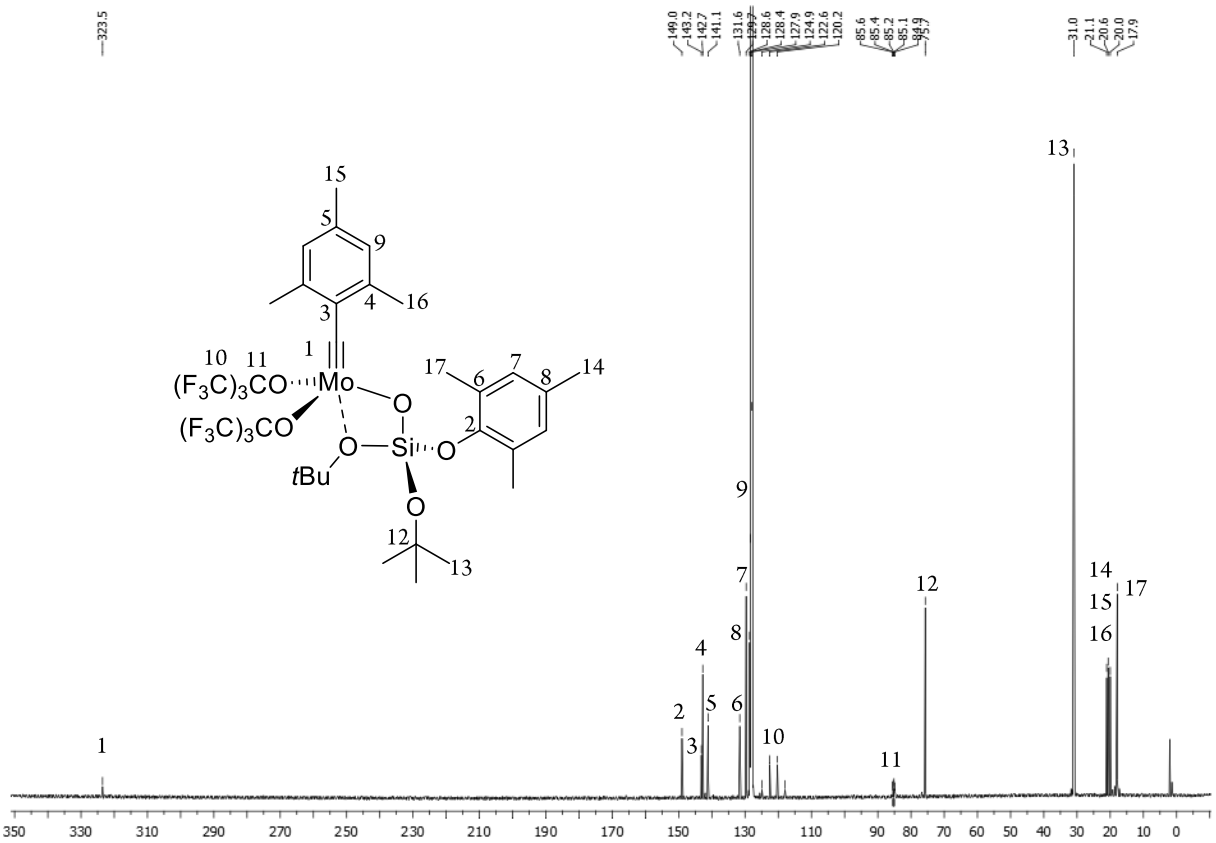


*Figure S14.* $^{13}C\{^{1}H\}$ *NMR spectrum of* ***MoSi*F9*** *in* $C_6D_6$.

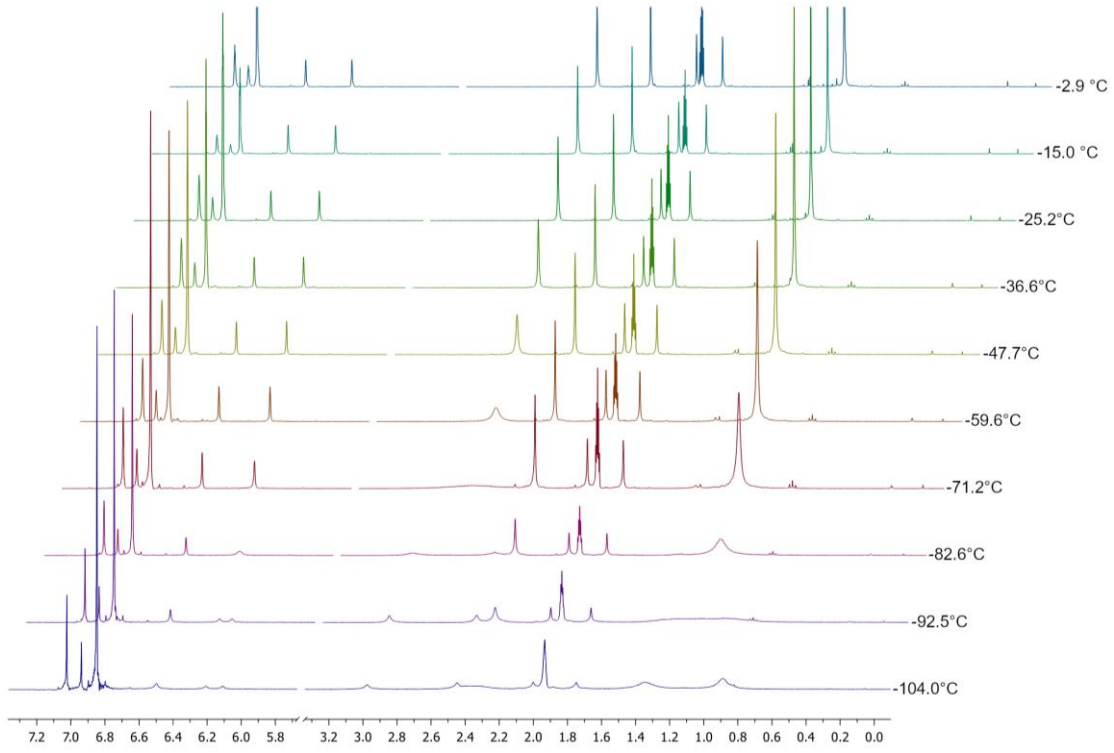


*Figure S15:* $^{1}H$ *variable temperature NMR spectra of* ***MoSi*F9*** *in toluene-*$d_8$.

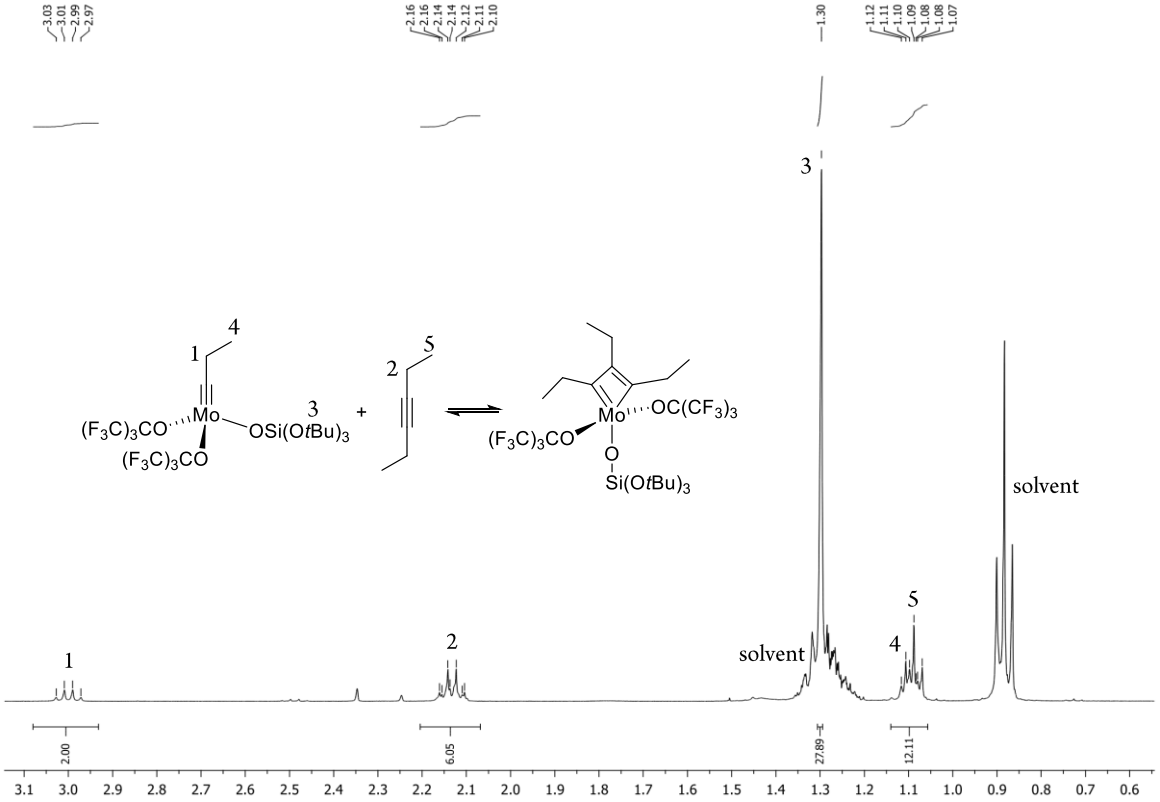


*Figure S16. $^{1}H$ NMR of **MoSiF9-MCBD** from 3.1–0.6 ppm in $CD_2Cl_2$ at rt. Only 3-hexyne and $^{Et}$**MoSiF9** visible.*

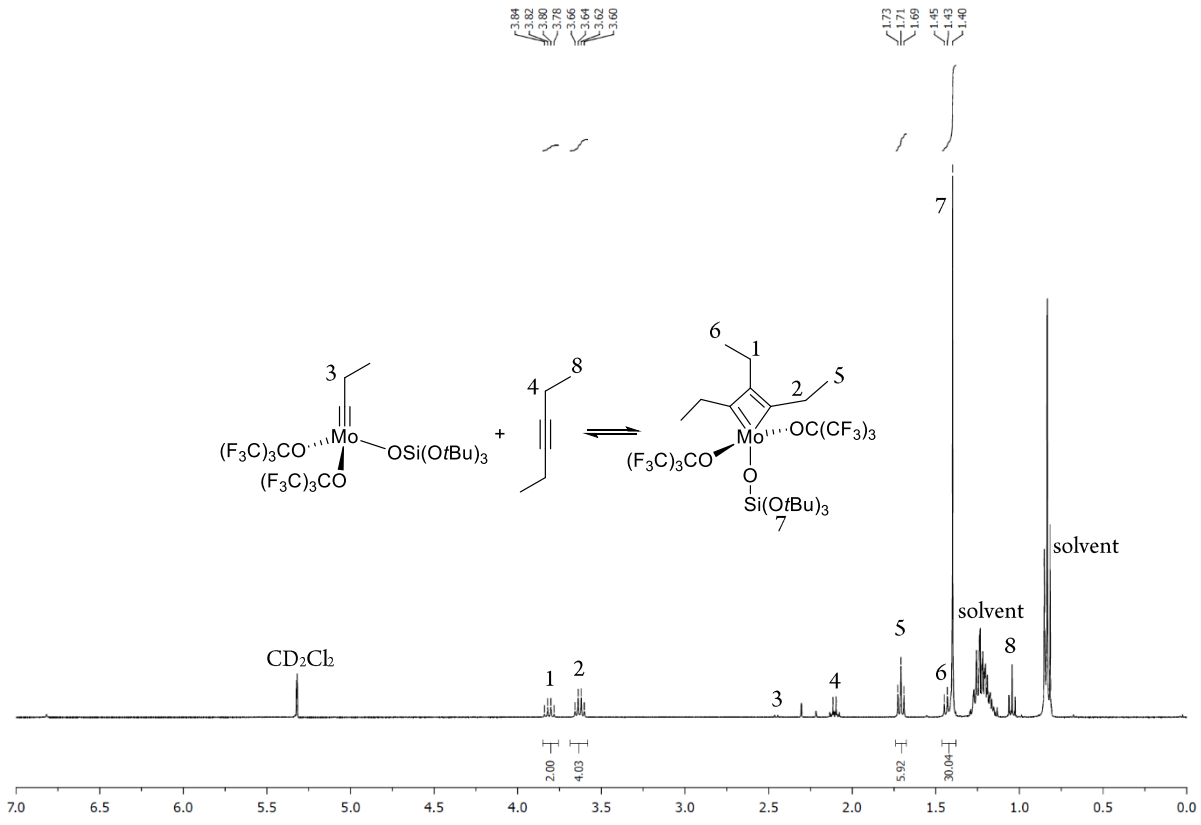


*Figure S17. $^{1}H$ NMR of **MoSiF9-MCBD** in $CD_2Cl_2$ at −39.6 °C.*

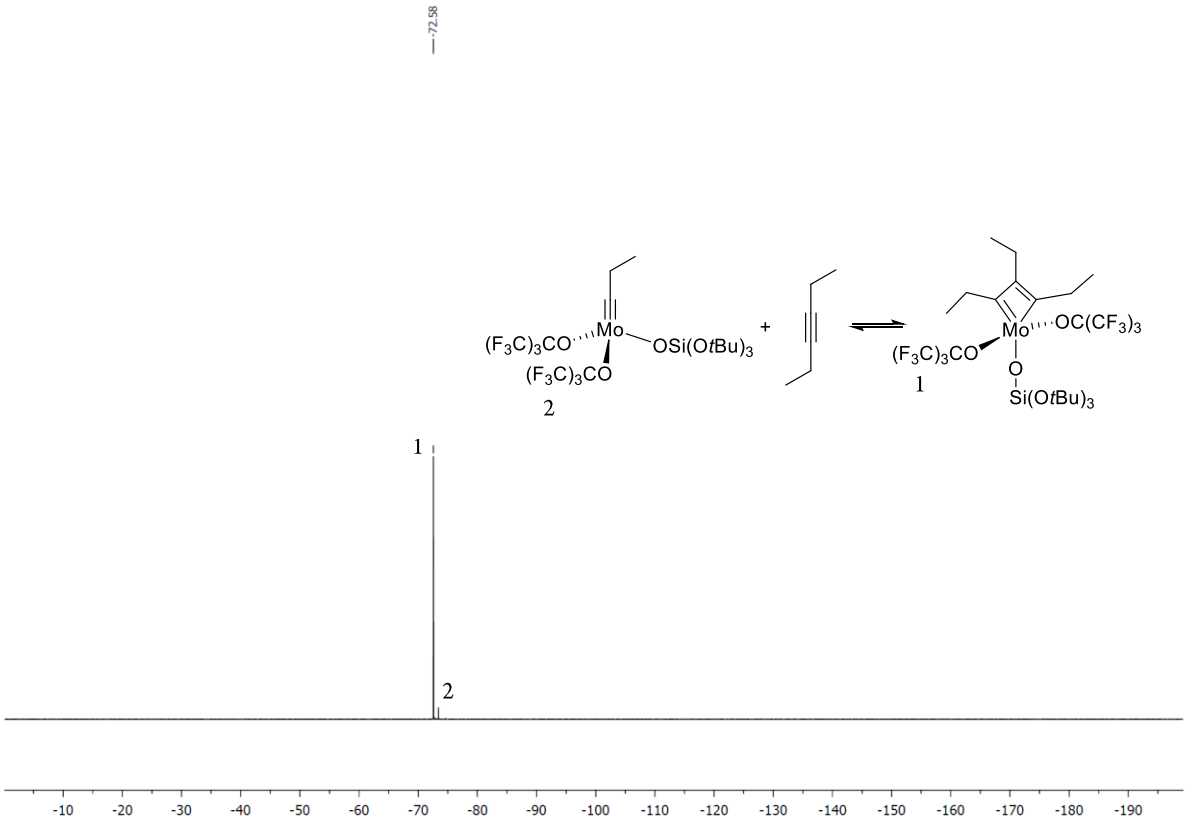


*Figure S18.* $^{19}F\{^{1}H\}$ *NMR of* ***MoSiF9-MCBD*** *in* $CD_2Cl_2$ *at –39.6 °C.*

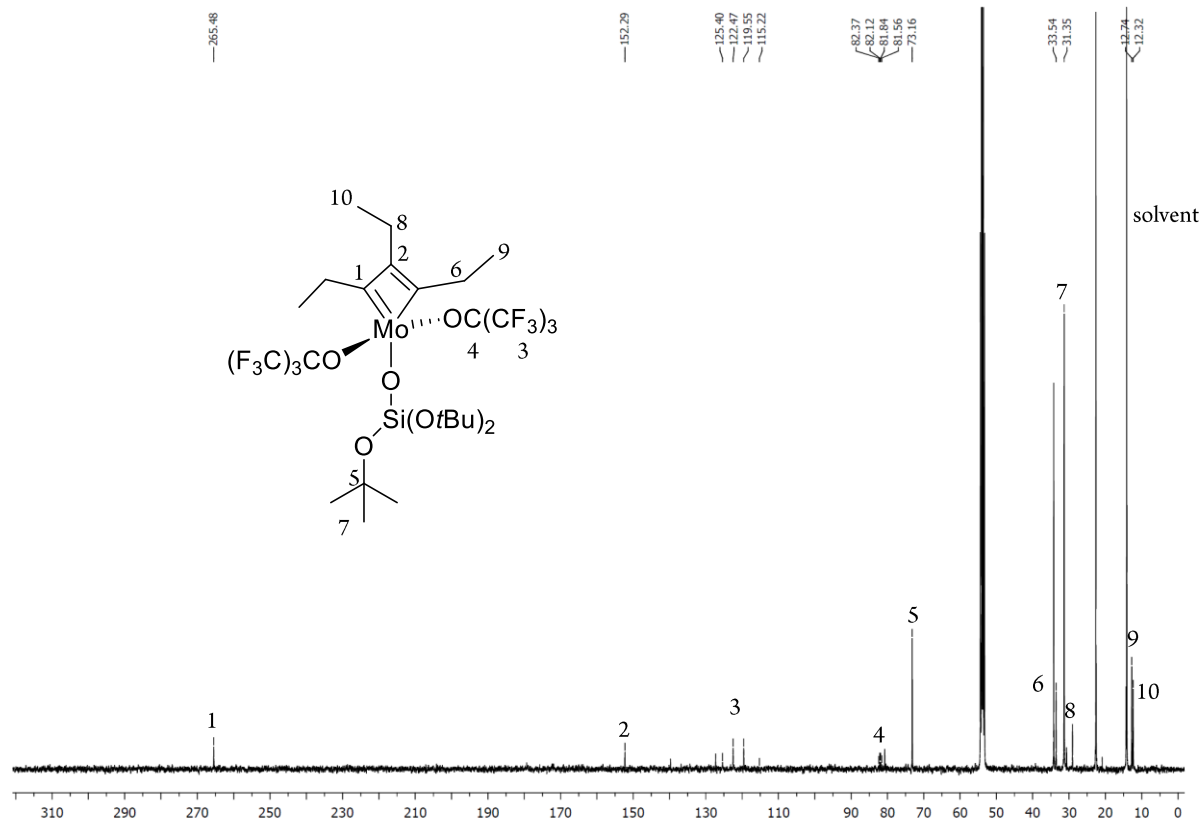


*Figure S19.* $^{13}C\{^{1}H\}$ *NMR of* ***MoSiF9-MCBD*** *in* $CD_2Cl_2$ *at –39.6 °C.*

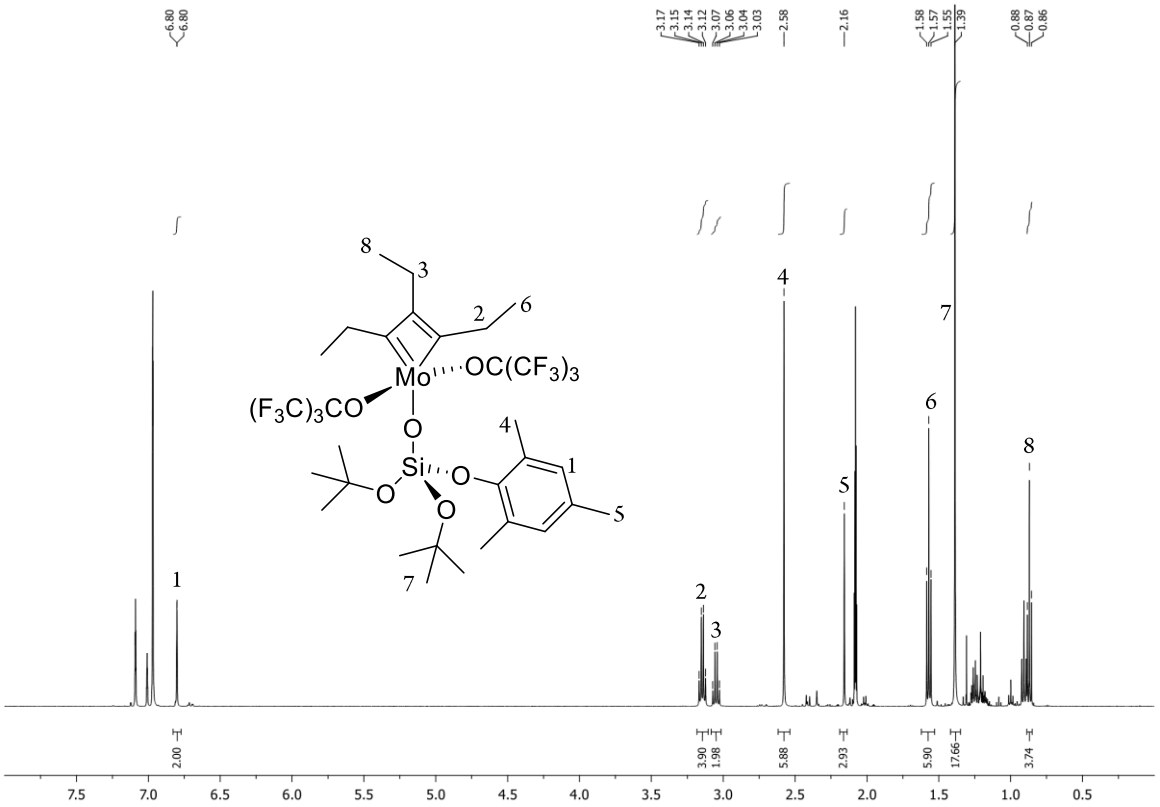

*Figure S20. $^{1}H$ NMR of **MoSi*F9-MCBD** in toluene-$d_8$ at rt.*

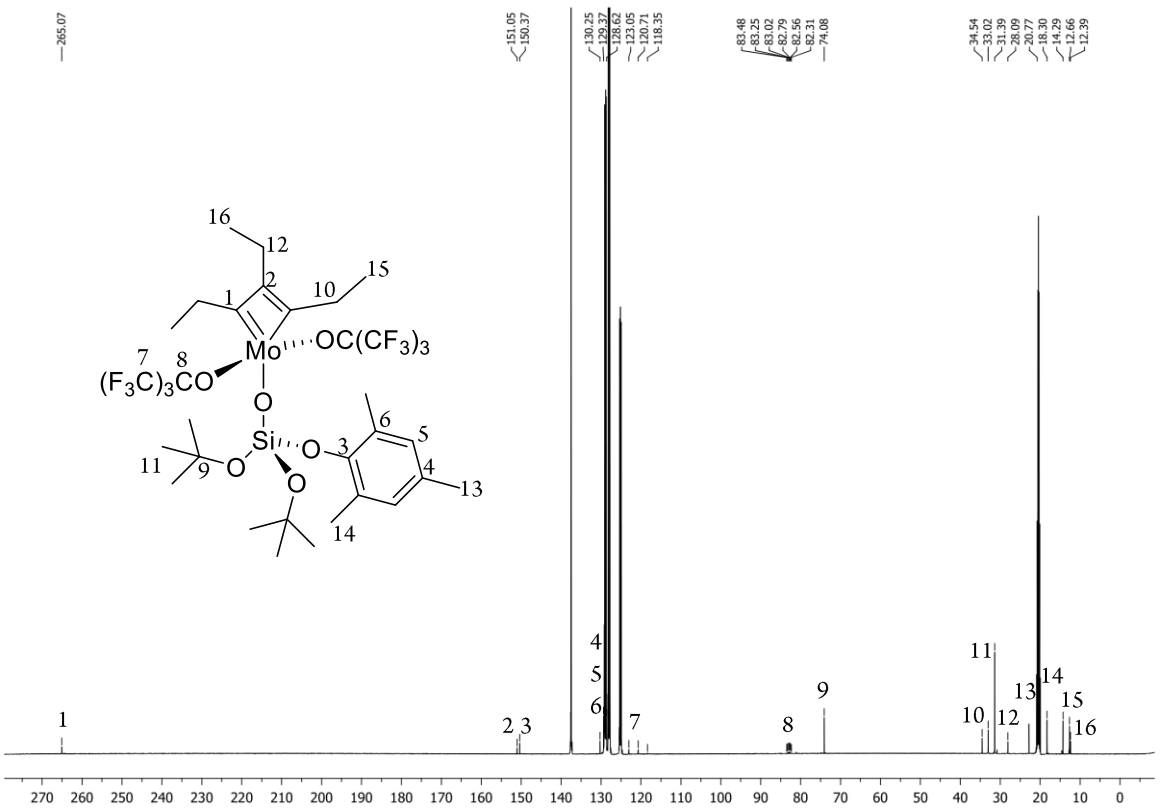

*Figure S21. $^{13}C\{^{1}H\}$ NMR of **MoSi*F9-MCBD** in toluene-$d_8$ at rt.*

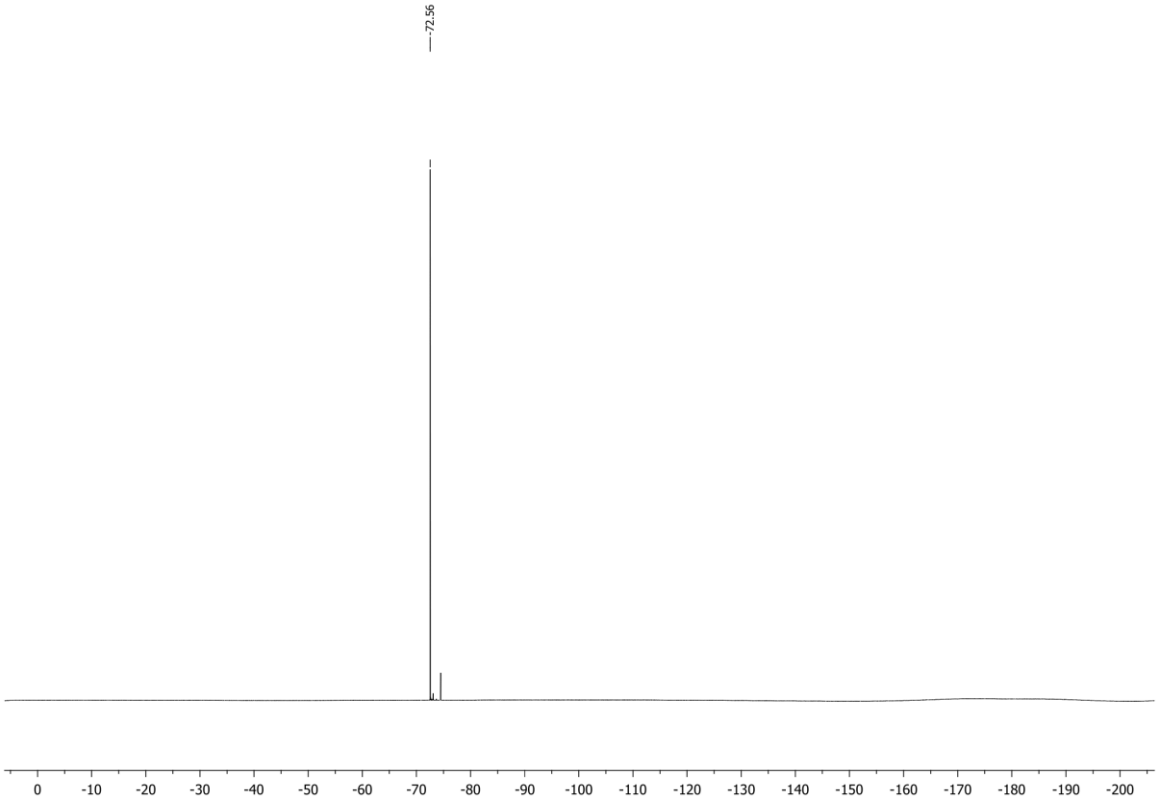


*Figure S22.* $^{19}F\{^{1}H\}$ *NMR of* ***MoSi*F9-MCBD*** *in toluene-*$d_8$ *at rt.*

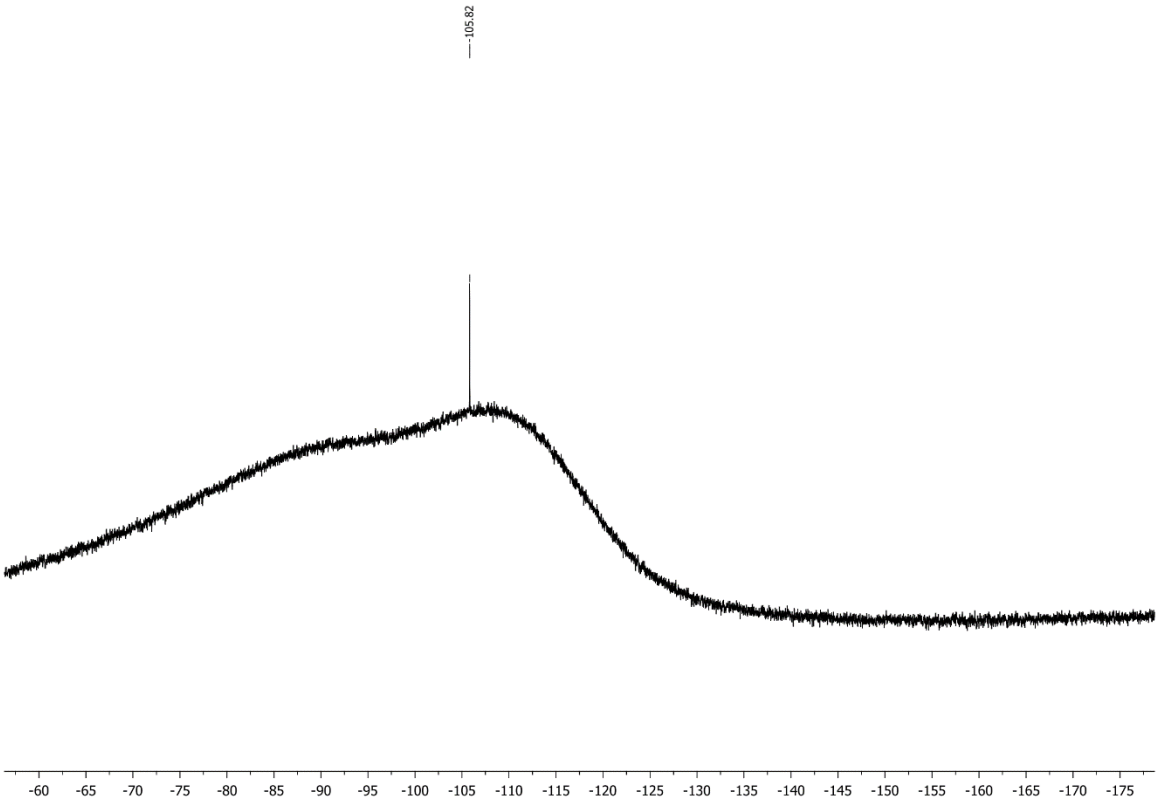


*Figure S23.* $^{29}Si$ *NMR* ***MoSi*F9-MCBD*** *in toluene-*$d_8$ *at rt.*

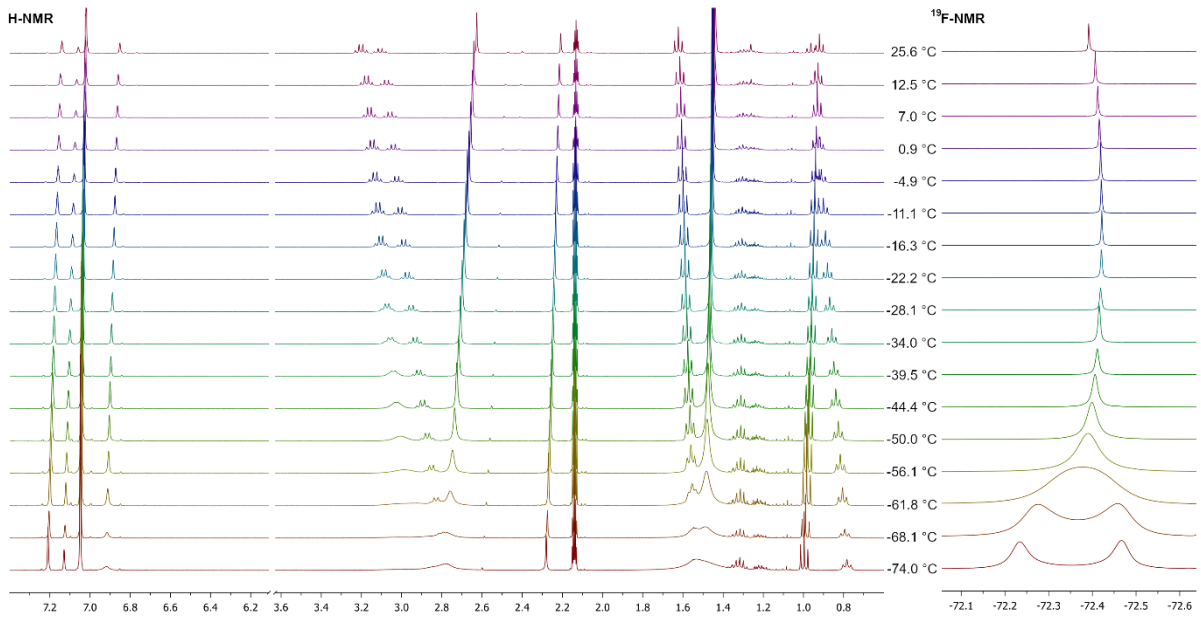


*Figure S24: $^{1}H$ and $^{19}F\{^{1}H\}$ variable temperature NMR spectra of* ***MoSi*F9-MCBD*** *in toluene-d₈.*

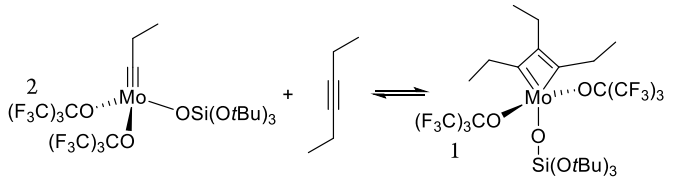


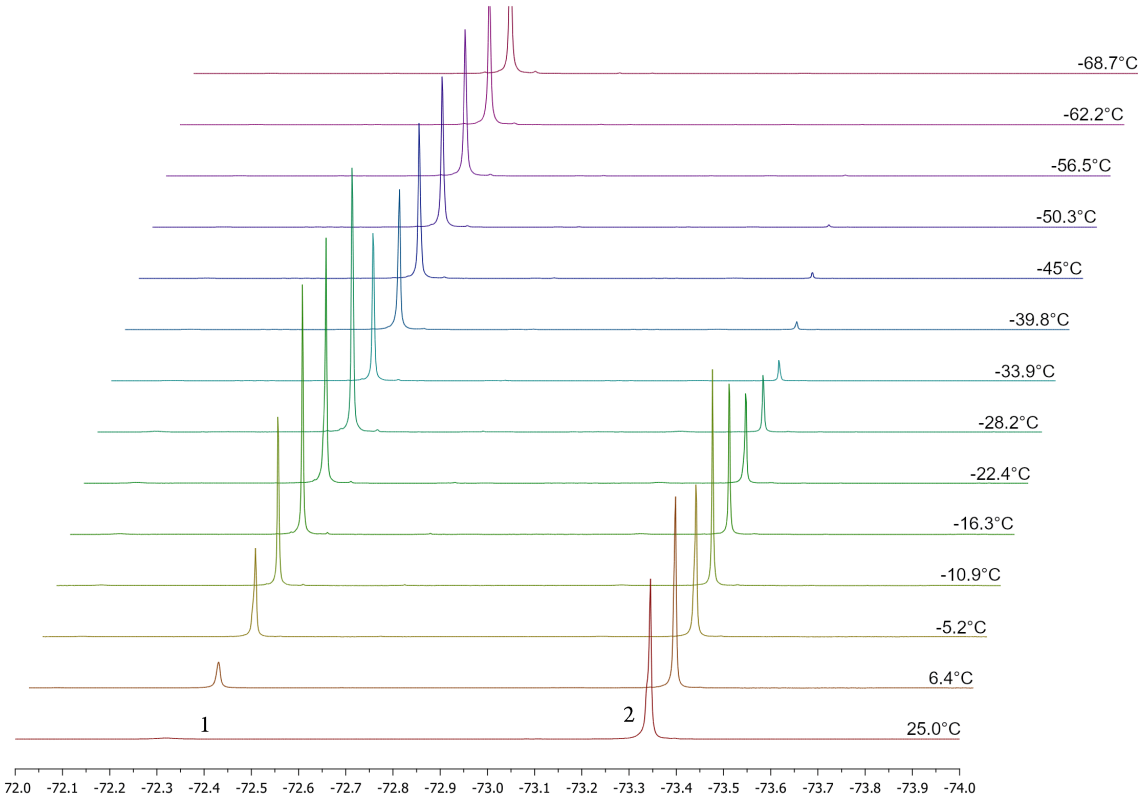


*Figure S25. $^{19}F\{^{1}H\}$ variable temperature NMR in $CD_2Cl_2$ used for VAN'T HOFF analysis. Left:* ***MoSiF9-MCBD****; right:* ***MoSiF9$^{Et}$****.*

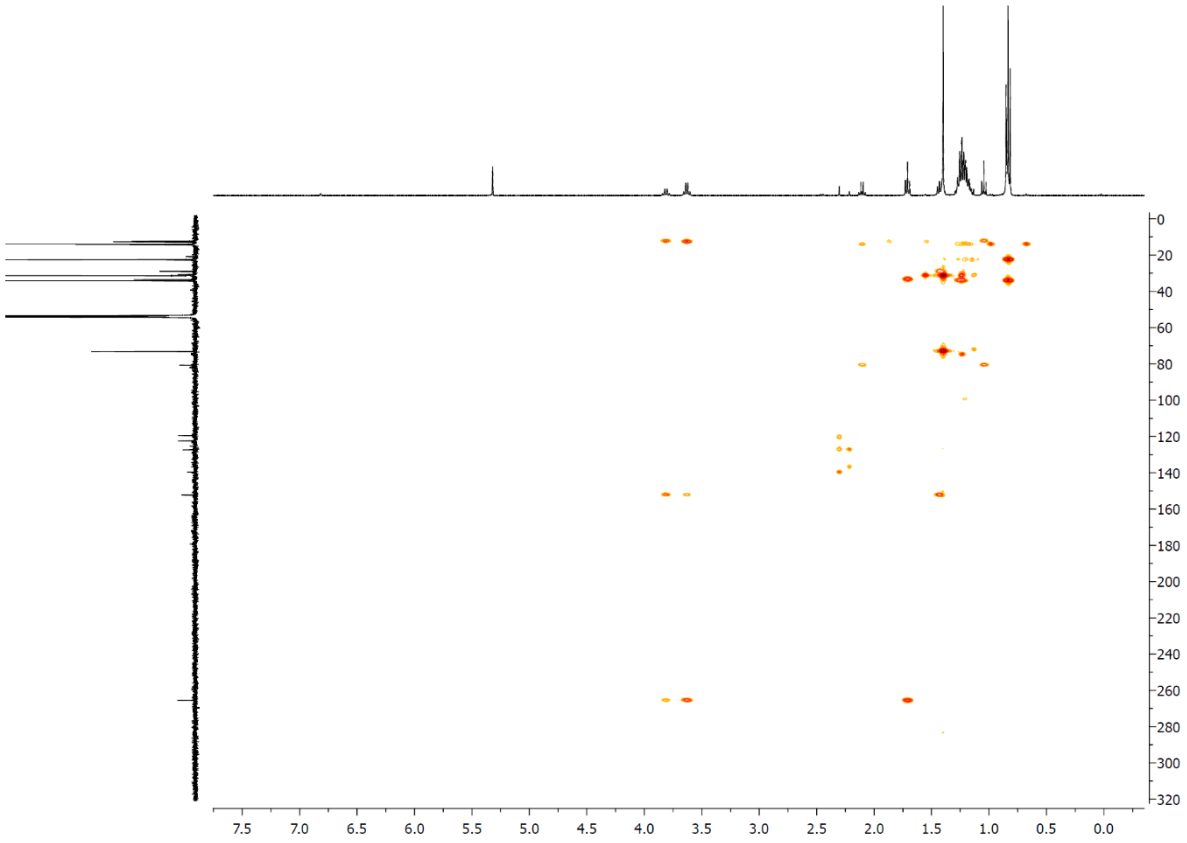


*Figure S26. HMBC from* ***MoSiF9-MCBD*** *at −39.6 °C in* $CD_2Cl_2$.

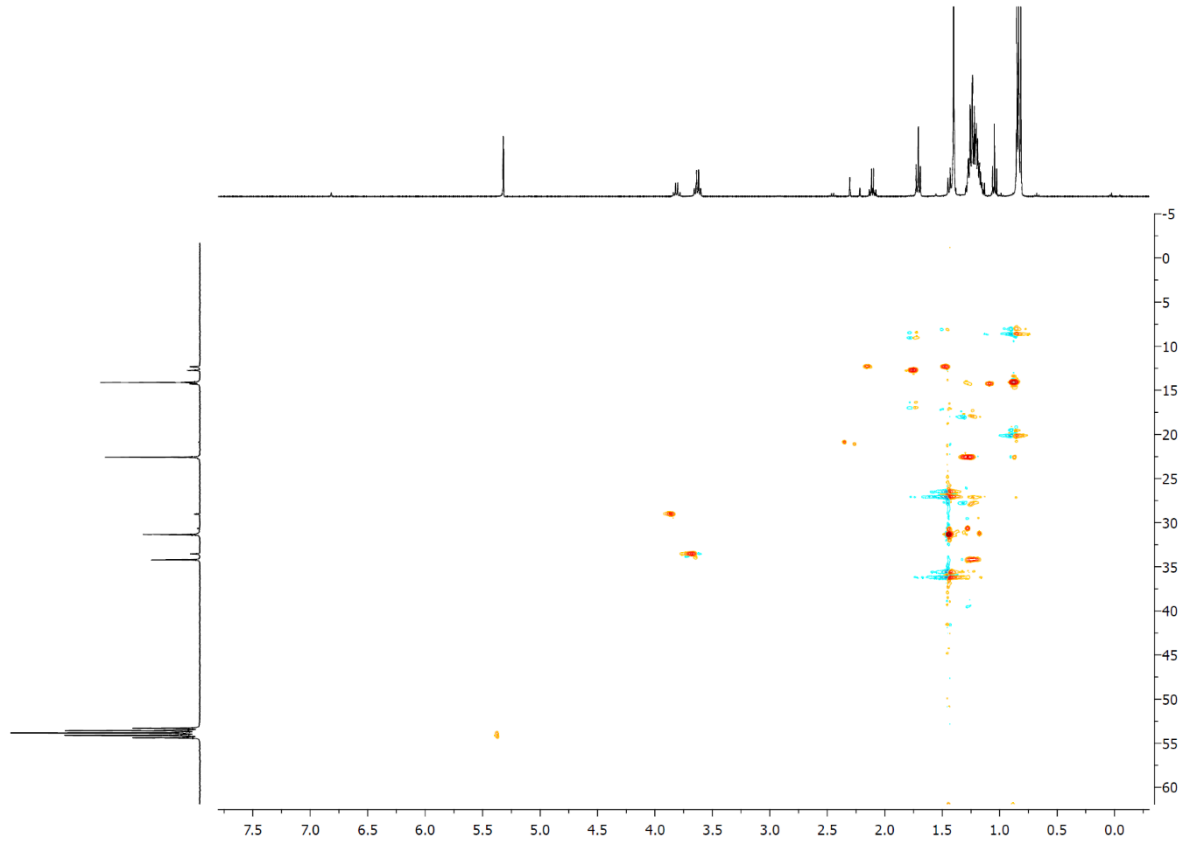


*Figure S27. HSQC from* ***MoSiF9-MCBD*** *at −39.6 °C in* $CD_2Cl_2$.

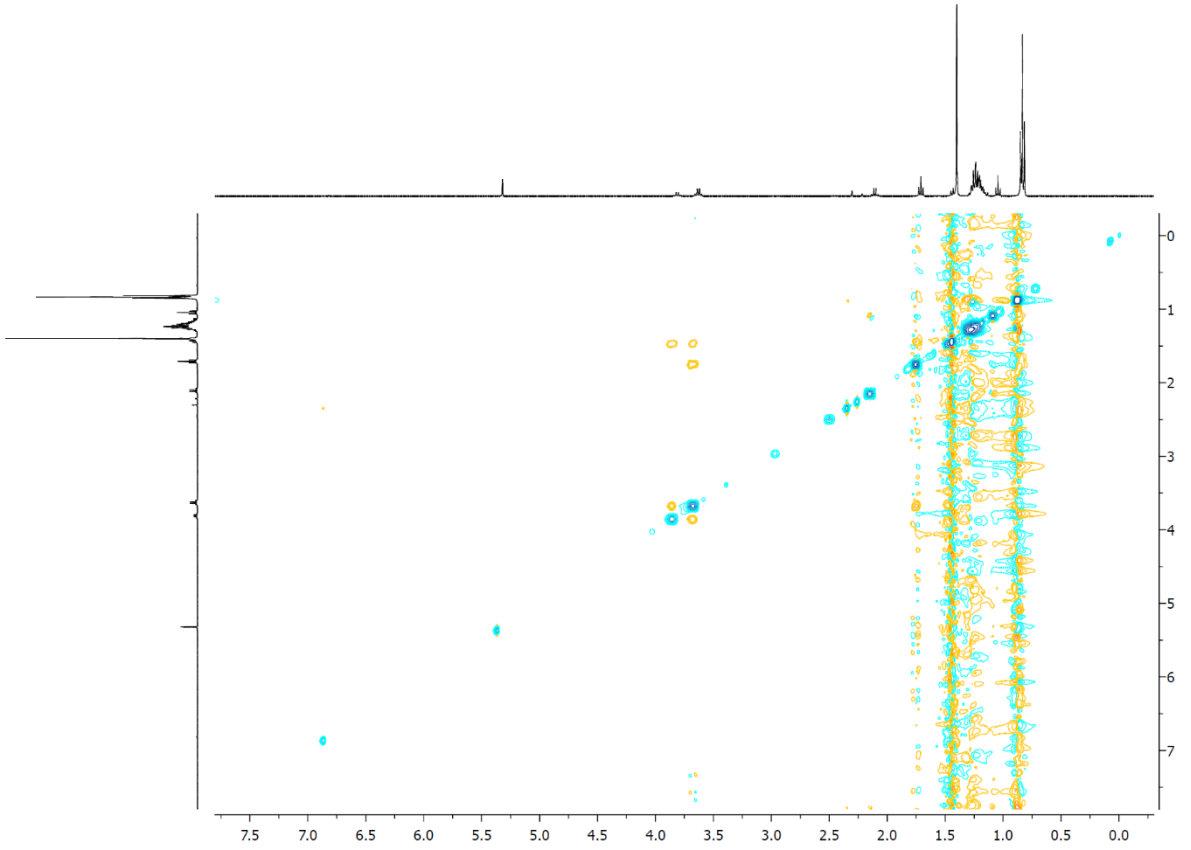


*Figure S28. NOESY from* ***MoSiF9-MCBD*** *at −39.6 °C in* $CD_2Cl_2$.

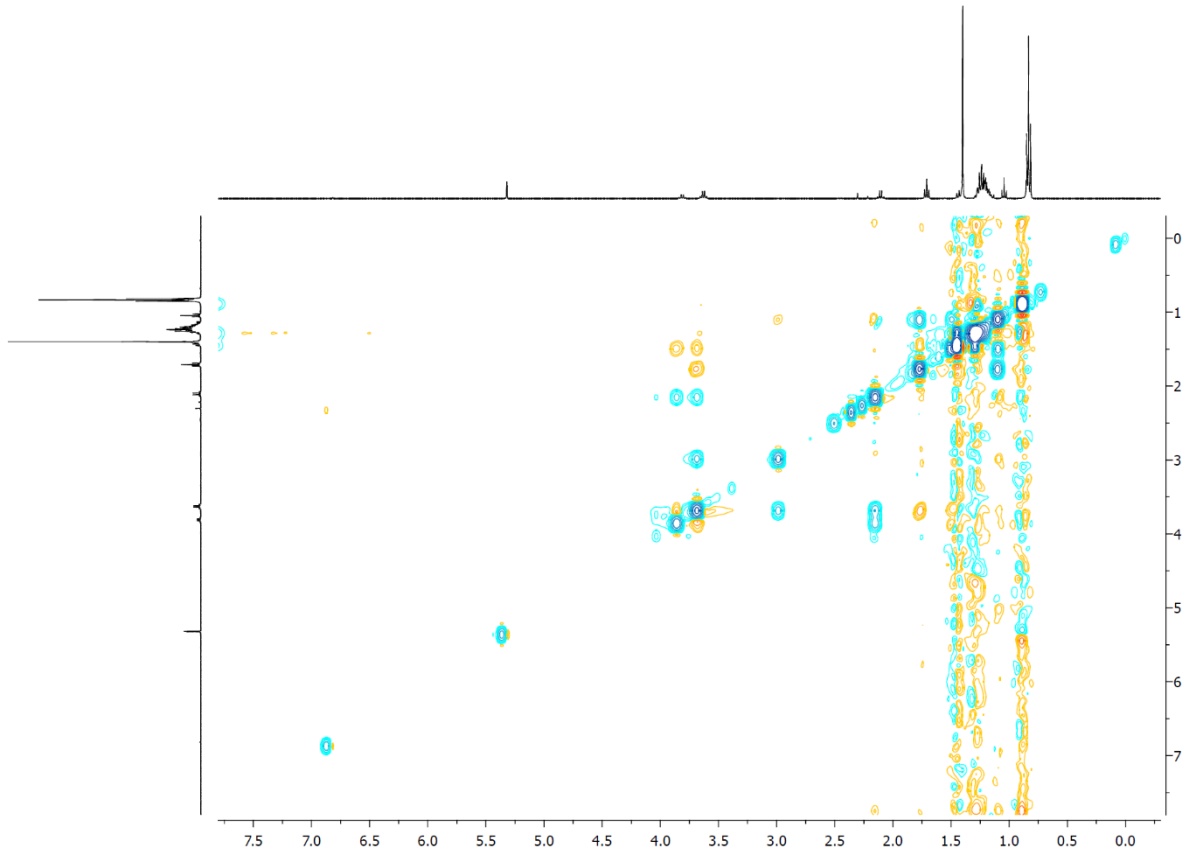


*Figure S29. NOESY from* ***MoSiF9-MCBD*** *at −17.0 °C in* $CD_2Cl_2$.

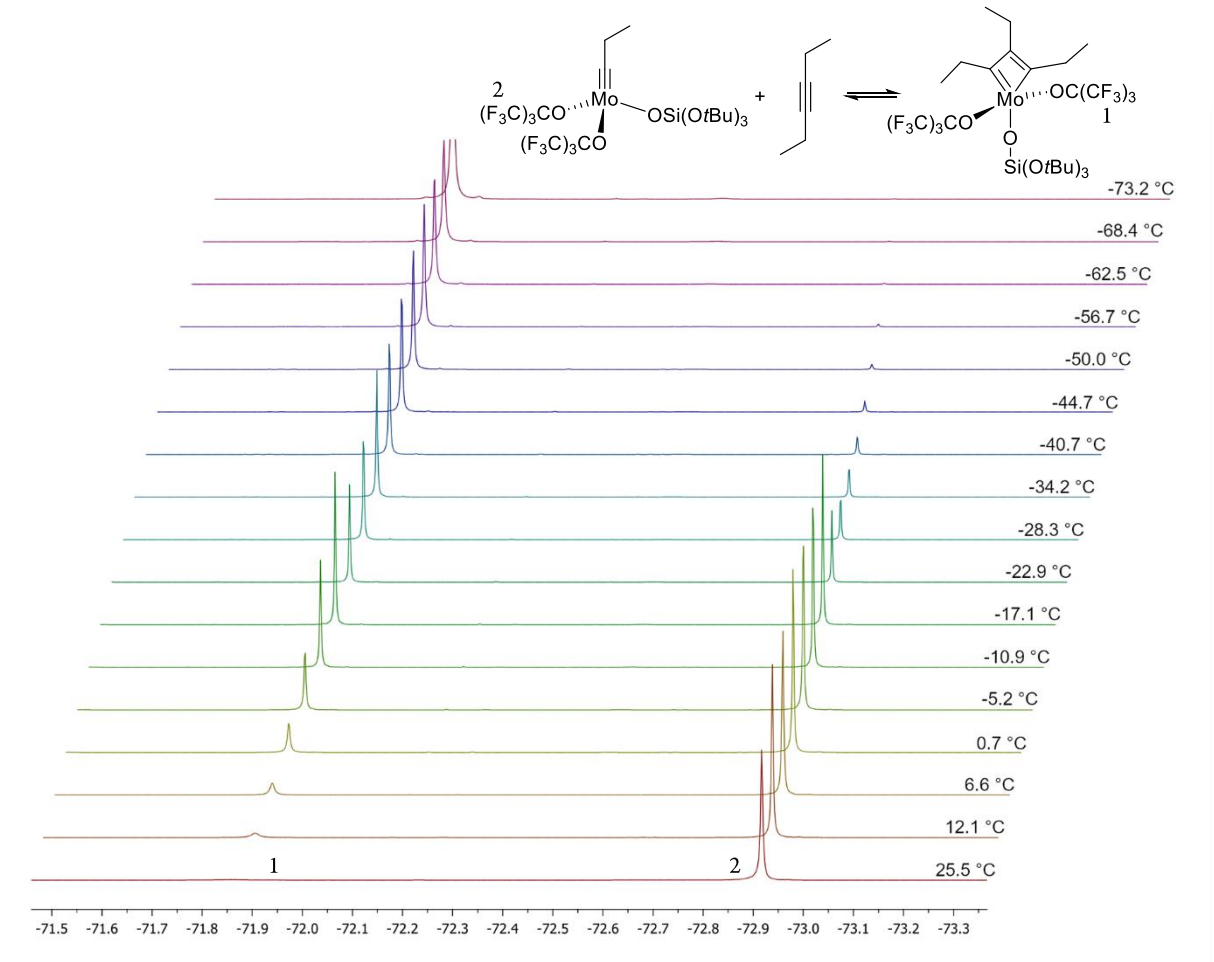


*Figure S30.* $^{19}F\{^{1}H\}$ *variable temperature NMR in toluene-*$d_8$ *used for* VAN'T HOFF *analysis. Left:* ***MoSiF9-MCBD****; right* ***MoSiF9$^{Et}$****.*

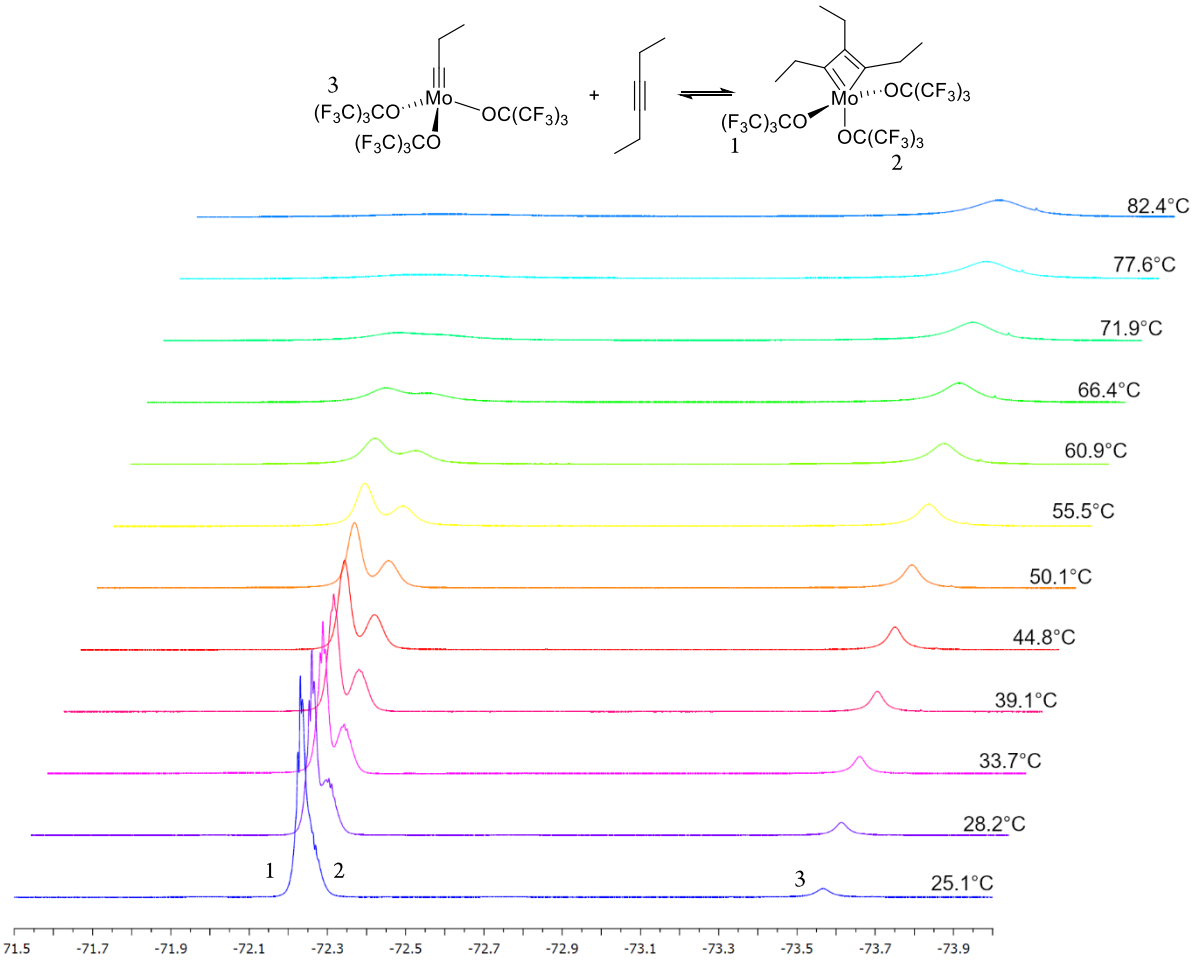


*Figure S31.* $^{19}F\{^{1}H\}$ *variable temperature NMR in toluene-*$d_8$ *used for* VAN'T HOFF *analysis. Left:* ***MoF9-MCBD****; right:* ***MoF9*** $^{Et}$.

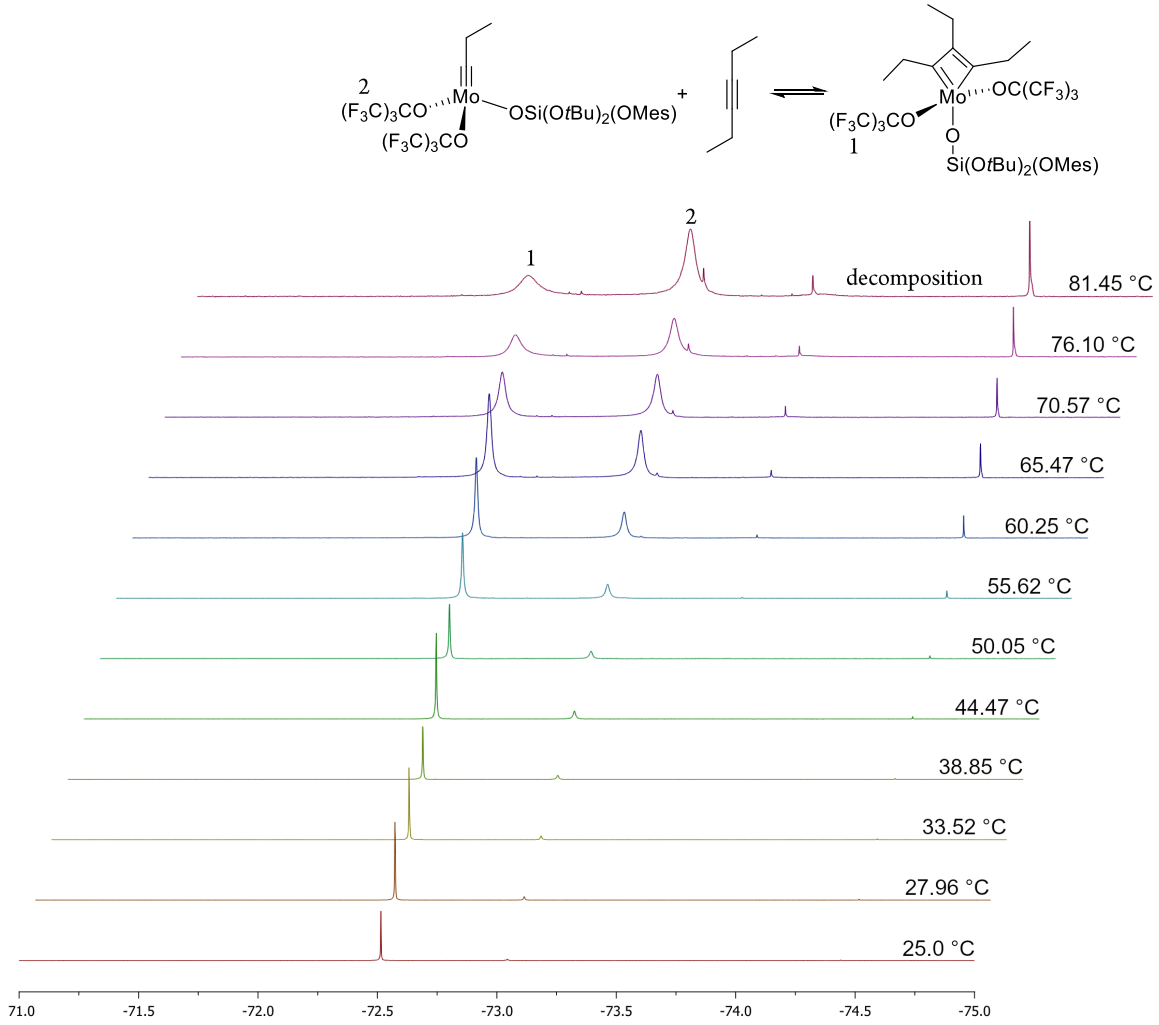


*Figure S32.* $^{19}F\{^{1}H\}$ *variable temperature NMR in toluene-*$d_8$ *used for* VAN'T HOFF *analysis. –72.51 ppm:* ***MoSi*F9-MCBD****, –73.04 ppm:* ***MoSi*F9***$^{Et}$.

## Van ’t Hoff Analysis

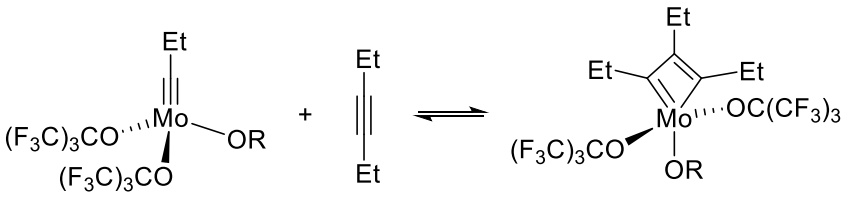


| alkylidyne | MCBD | R |
|---|---|---|
| **MoF9$^{Et}$** | **MoF9-MCBD** | $C(CF_3)_3$ |
| **MoSiF9$^{Et}$** | **MoSiF9-MCBD** | $Si(OtBu)_3$ |
| **MoSi*F9$^{Et}$** | **MoSi*F9-MCBD** | $Si(OtBu)_2(OMes)$ |

*Scheme S1. [2+2]-cycloreversion of the respective MCBD.*

The metallacycle **MoF9-MCBD**, **MoSiF9-MCBD** or **MoSi*F9-MCBD** were dissolved in toluene-$d_8$ (also $CD_2Cl_2$ for **MoSiF9-MCBD**) and transferred to an NMR tube. The NMR tube was inserted into a temperature-controlled NMR spectrometer and $^1$H NMR and $^{19}$F{$^1$H} NMR spectra were recorded in a specific temperature range. The ratio of alkylidyne and MCBD was determined by integration of the $^{19}$F{$^1$H} NMR resonances and the amount of 3-hexyne must be equal to the respective alkylidyne. The equilibrium constants at different temperatures were calculated according to the following formula:

$$K_{eq} = \frac{[\text{MCBD}]}{[\text{Alkylidyne}]^2}$$

Subsequently, $\ln(K_{eq})$ was plotted as a function of $1/T$ and according to the following formula the enthalpy, entropy of the reaction could be extracted from the slope and the y-axis intercept of the linear fit:

$$\ln(K_{eq}) = \frac{-\Delta H}{R} \cdot \frac{1}{T} + \frac{\Delta S}{R}$$

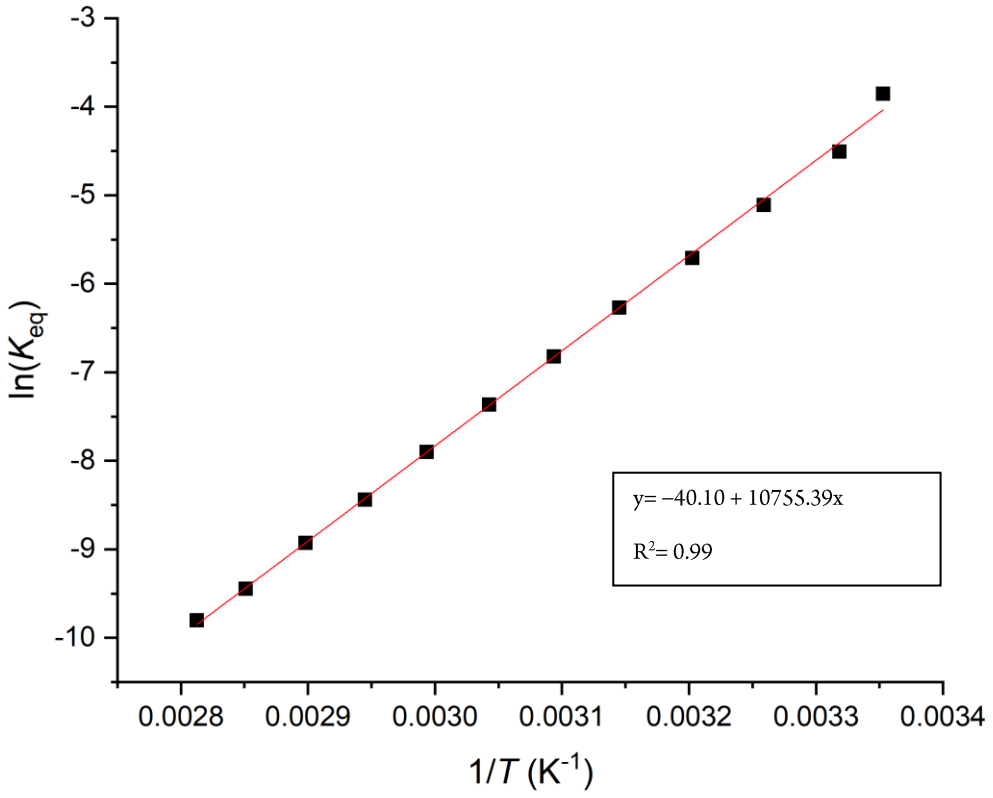


*Figure S33. VAN 'T HOFF plot of the [2+2]-cycloreversion of **MoF9-MCBD** derived from $^{19}F\{^1H\}$ NMR spectroscopic data in toluene-$d_8$ from 298.25 K to 355.75 K in ~5 K intervals.*

*Table S1. Data points used for the van 't Hoff analysis of the [2+2]-cycloreversion of **MoF9-MCBD** in toluene-$d_8$.*

| | Col(A) | Col(B) | Col(C) | Col(D) | Col(E) | Col(F) | Col(G) |
|---|---|---|---|---|---|---|---|
| | | | | Integral | Integral | | |
| | temperature [°C] | temperature [K] | 1/T | MCBD | Alkylidyne | K | ln(K) |
| **function** | | (Col(A)) +273.15 | 1/(Col(B)) | | | Col(D)/(Col(E)^2) | ln(Col(F)) |
| **1** | 25.1 | 298.25 | 0.00335 | 9336.36 | 663.64 | 0.0212 | −3.85381 |
| **2** | 28.2 | 301.35 | 0.00332 | 9092.17 | 907.83 | 0.01103 | −4.50695 |
| **3** | 33.7 | 306.85 | 0.00326 | 8792.21 | 1207.79 | 0.00603 | −5.11147 |
| **4** | 39.1 | 312.25 | 0.0032 | 8406.69 | 1593.31 | 0.00331 | −5.71035 |
| **5** | 44.8 | 317.95 | 0.00315 | 7951.93 | 2048.07 | 0.0019 | −6.26814 |
| **6** | 50.1 | 323.25 | 0.00309 | 7395.92 | 2604.08 | 0.00109 | −6.82099 |
| **7** | 55.5 | 328.65 | 0.00304 | 6736.3 | 3263.7 | 6.32413E-4 | −7.36597 |
| **8** | 60.9 | 334.05 | 0.00299 | 5984.94 | 4015.06 | 3.71258E-4 | −7.89861 |
| **9** | 66.4 | 339.55 | 0.00295 | 5131.3 | 4868.7 | 2.16472E-4 | −8.43805 |
| **10** | 71.9 | 345.05 | 0.0029 | 4302.65 | 5697.35 | 1.32553E-4 | −8.92853 |
| **11** | 77.6 | 350.75 | 0.00285 | 3423.17 | 6576.83 | 7.91399E-5 | −9.44429 |
| **resulting linear plot function:** y = a+ b*x with a = −40.09847 ± 0.37065 and b = 10755.39235 ± 120.29497 | | | | | | | |

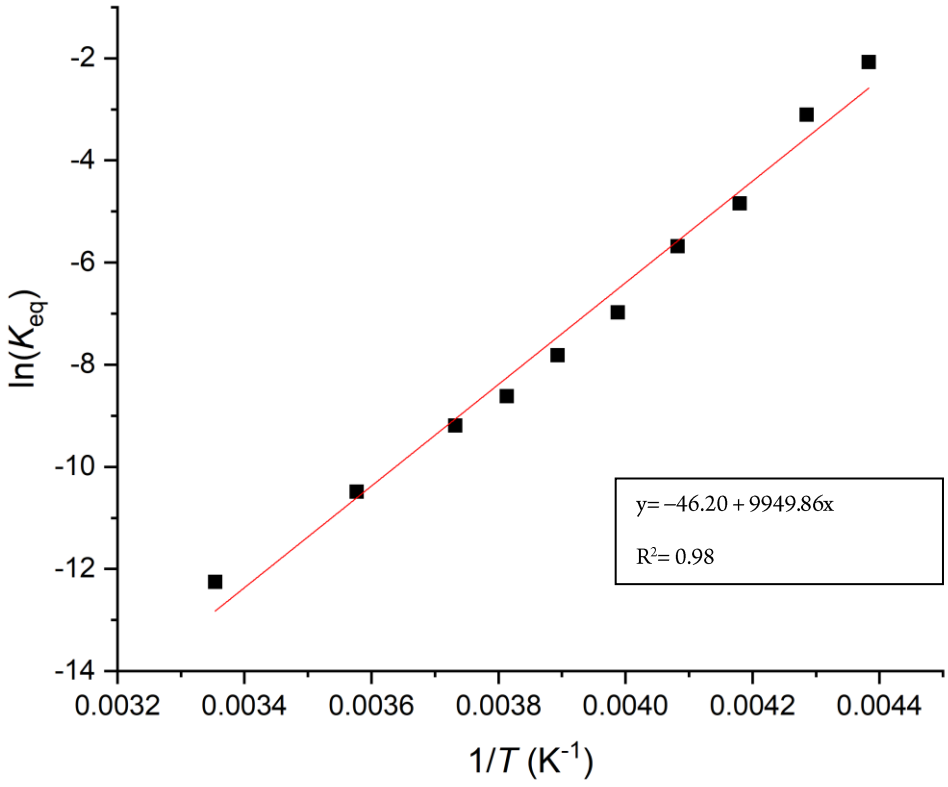


*Figure S34. VAN 'T HOFF plot of the [2+2]cycloreversion of* ***MoSiF9-MCBD****, derived from $^{19}F\{^1H\}$ NMR spectroscopic data in $CD_2Cl_2$ from 228.15 K to 298.15 K in ~5 K intervals.*

*Table S2. Data points used for the van 't Hoff analysis of the [2+2]-cycloreversion of* ***MoSiF9-MCBD*** *in $CD_2Cl_2$.*

| | **Col(A)** | **Col(B)** | **Col(C)** | **Col(D)** | **Col(E)** | **Col(F)** | **Col(G)** |
|---|---|---|---|---|---|---|---|
| | temperature [°C] | temperature [K] | 1/T | Integral MCBD | Integral Alkylidyne | K | ln(K) |
| **function** | | (Col(A))+273.15 | 1/(Col(B)) | | | Col(D)/(Col(E)^2) | ln(Col(F)) |
| **1** | −45.0 | 228.15 | 0.00438 | 9721.84 | 278.16 | 0.12565 | −2.07426 |
| **2** | −39.8 | 233.35 | 0.00429 | 9537.54 | 462.46 | 0.0446 | −3.11013 |
| **3** | −33.9 | 239.25 | 0.00418 | 8936.74 | 1063.26 | 0.0079 | −4.84026 |
| **4** | −28.2 | 244.95 | 0.00408 | 8426.83 | 1573.17 | 0.0034 | −5.68252 |
| **5** | −22.4 | 250.75 | 0.00399 | 7222.13 | 2777.87 | 9.35926E-4 | −6.97397 |
| **6** | −16.3 | 256.85 | 0.00389 | 6102.31 | 3897.69 | 4.0168E-4 | −7.81986 |
| **7** | −10.9 | 262.25 | 0.00381 | 4828.48 | 5171.52 | 1.8054E-4 | −8.61956 |
| **8** | −5.2 | 267.95 | 0.00373 | 3851.46 | 6148.54 | 1.01878E-4 | −9.19173 |
| **9** | 6.4 | 279.55 | 0.00358 | 1849.79 | 8150.21 | 2.78474E-5 | −10.48877 |
| **10** | 25.0 | 298.15 | 0.00335 | 437.25 | 9562.75 | 4.7815E-6 | −12.25076 |

**resulting linear plot function:** y = a+ b*x with a = −46.19661 ± 1.68231 and b = 9949.85681 ± 426.90919

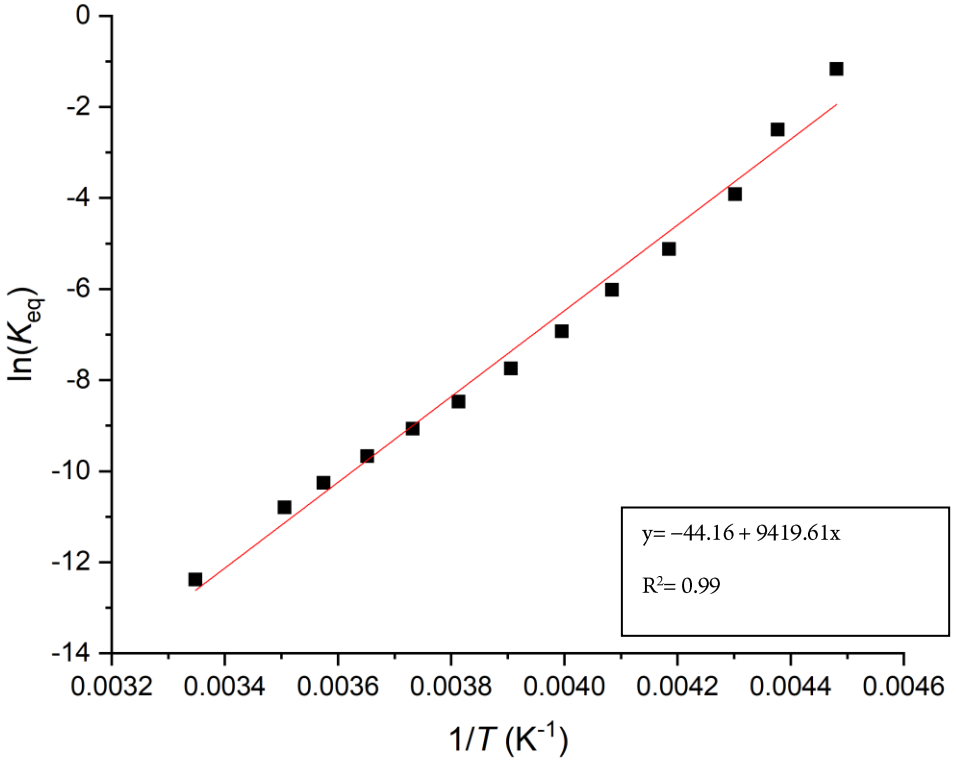


*Figure S35. VAN 'T HOFF plot of the [2+2]-cycloreversion of* ***MoSiF9-MCBD*** *derived from $^{19}F\{^{1}H\}$ NMR spectroscopic data in toluene-$d_8$ from 223.15 K to 298.65 K in ~5 K intervals.*

*Table S3. Data points used for the van 't Hoff analysis of the [2+2]-cycloreversion* ***MoSiF9-MCBD*** *in toluene-$d_8$.*

| | **Col(A)** | **Col(B)** | **Col(C)** | **Col(D)** | **Col(E)** | **Col(F)** | **Col(G)** |
|---|---|---|---|---|---|---|---|
| | | | | Integral | Integral | | |
| | temperature [°C] | temperature [K] | 1/T | MCBD | Alkylidyne | K | lnK |
| **function** | | (Col(A))+ 273.15 | 1/(Col(B)) | | | Col(D)/(Col(E)^ 2) | ln(Col(F)) |
| **1** | −50.0 | 223.15 | 0.00448 | 9822.55 | 177.45 | 0.31194 | −1.16494 |
| **2** | −44.7 | 228.45 | 0.00438 | 9656.77 | 343.23 | 0.08197 | −2.50139 |
| **3** | −40.7 | 232.45 | 0.0043 | 9315.49 | 684.51 | 0.01988 | −3.91797 |
| **4** | −34.2 | 238.95 | 0.00418 | 8785.33 | 1214.67 | 0.00595 | −5.12362 |
| **5** | −28.3 | 244.85 | 0.00408 | 8167.07 | 1832.93 | 0.00243 | −6.01948 |
| **6** | −22.9 | 250.25 | 0.004 | 7277.44 | 2722.56 | 9.81802E-4 | −6.92612 |
| **7** | −17.1 | 256.05 | 0.00391 | 6210.94 | 3789.06 | 4.32608E-4 | −7.74568 |
| **8** | −10.9 | 262.25 | 0.00381 | 5069.14 | 4930.86 | 2.08492E-4 | −8.47561 |
| **9** | −5.2 | 267.95 | 0.00373 | 4064.54 | 5935.46 | 1.15373E-4 | −9.06734 |
| **10** | 0.7 | 273.85 | 0.00365 | 3048.23 | 6951.77 | 6.3075E-5 | −9.67119 |
| **11** | 6.6 | 279.75 | 0.00357 | 2156.8 | 7843.2 | 3.50609E-5 | −10.25842 |
| **12** | 12.1 | 285.25 | 0.00351 | 1484.29 | 8515.71 | 2.04681E-5 | −10.79664 |
| **13** | 25.5 | 298.65 | 0.00335 | 387.99 | 9612.01 | 4.19945E-6 | −12.38056 |
| **resulting linear plot function:** y = a + b*x with a = −44.15707 ± 1.2696 and b = 9419.61241 ± 332.68096 | | | | | | | |

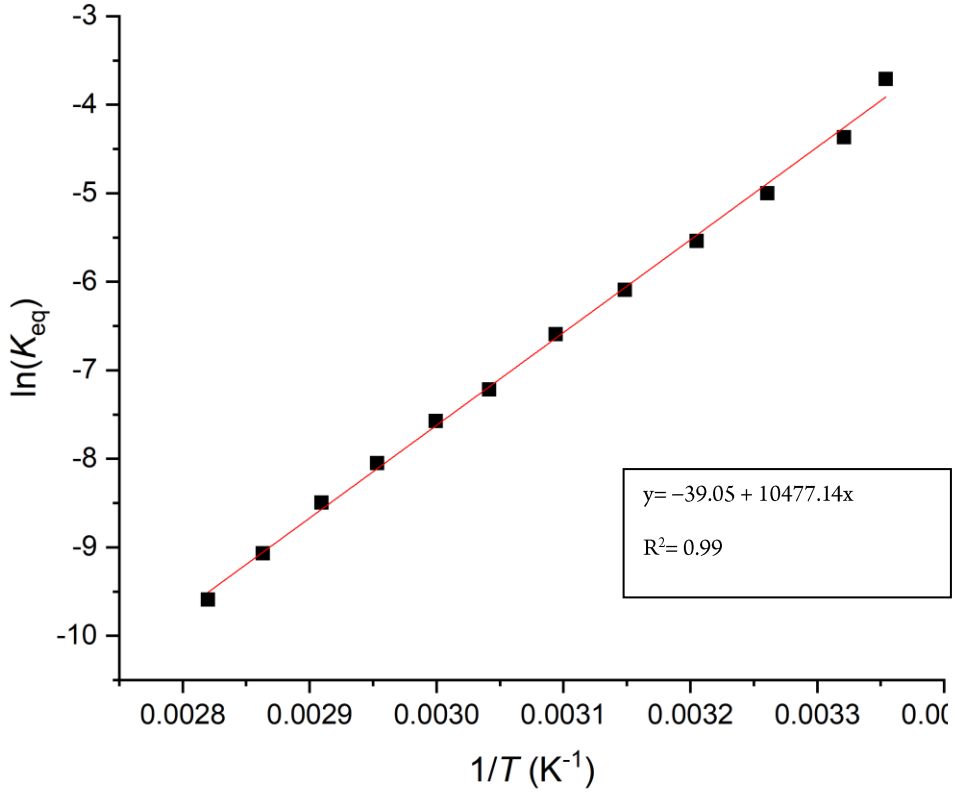


*Figure S36. VAN 'T HOFF plot of the [2+2]-cycloreversion of **MoSi*F9-MCBD** derived from $^{19}F\{^{1}H\}$ NMR spectroscopic data in toluene-$d_8$ from 298.15 K to 354.60 K in ~5 K intervals.*

*Table S4. Data points used for the van 't Hoff analysis of the [2+2]-cycloreversion of **MoSi*F9-MCBD** in toluene-$d_8$.*

| | **Col(A)** | **Col(B)** | **Col(C)** | **Col(D)** | **Col(E)** | **Col(F)** | |
|---|---|---|---|---|---|---|---|
| | | | | Integral | Integral | | |
| | temperature [°C] | temperature [K] | 1/T | MCBD | Alkylidyne | K | lnK |
| **function** | | (Col(A)) +273.15 | 1/(Col(B)) | | (Col(D))^2 | Col(D)/(Col(E)^2) | ln(Col(F)) |
| **1** | 25.00 | 298.15 | 0.00335 | 9380.85 | 619.15 | 0.02447 | −3.71027 |
| **2** | 27.96 | 301.11 | 0.00332 | 9150.91 | 849.09 | 0.01269 | −4.36672 |
| **3** | 33.52 | 306.67 | 0.00326 | 8852.46 | 1147.54 | 0.00672 | −5.0023 |
| **4** | 38.85 | 312.00 | 0.00321 | 8527.1 | 1472.9 | 0.00393 | −5.53897 |
| **5** | 44.47 | 317.62 | 0.00315 | 8105.32 | 1894.68 | 0.00226 | −6.09333 |
| **6** | 50.05 | 323.20 | 0.00309 | 7638.48 | 2361.52 | 0.00137 | −6.59317 |
| **7** | 55.62 | 328.77 | 0.00304 | 6929.1 | 3070.9 | 7.3476E-4 | −7.21597 |
| **8** | 60.25 | 333.40 | 0.003 | 6452.99 | 3547.01 | 5.12904E-4 | −7.57542 |
| **9** | 65.47 | 338.62 | 0.00295 | 5754.03 | 4245.97 | 3.19167E-4 | −8.0498 |
| **10** | 70.57 | 343.72 | 0.00291 | 5038.38 | 4961.62 | 2.04665E-4 | −8.49414 |
| **11** | 76.10 | 349.25 | 0.00286 | 4061.75 | 5938.25 | 1.15185E-4 | −9.06897 |
| **12** | 81.45 | 354.60 | 0.00282 | 3180.12 | 6819.88 | 6.83739E-5 | −9.59052 |

**resulting linear plot function:** y = a + b*x with a = −39.05363 ± 0.50118 and b = 10477.13527 ± 162.42408

## XRD details

Crystals were mounted with per-fluorinated inert oil. Data were recorded on Oxford Diffraction Xcalibur diffractometers with monochromated Mo-Kα radiation and an EOS CCD detector (**MoSiF0**, **MoSiF3**, **MoSi2F9**) or mirror focussed Cu-Kα radiation and an ATLAS CCD detector (**MoSiF9**, **MoSiF9-MCBD**). Additionally, Rigaku XtaLAB Synergy S Single Source diffractometers equipped with a PhotonJet Cu-microfocus source (**MoSi*F9**) or a PhotonJet Mo-microfocus source (**MoSi*F9-MCBD**) and a HyPix-6000HE detector. Data reduction was performed with CrysalisPro[5]. Absorption correction was based on multi-scans and for some crystals (**MoSiF9**, **MoSi*F9**, **MoSiF9-MCBD**, **MoSi*F9-MCBD**) additionally face indexation and integration on a Gaussian grid was applied. The structures were solved by direct methods with SHELXS[6] (**MoSiF0**, **MoSiF3**, **MoSi2F9**) or intrinsic phasing with SHELXT[7] (**MoSiF9**, **MoSi*F9**, **MoSiF9-MCBD**, **MoSi*F9-MCBD**) and refined on $F^2$ using the program SHELXL-2018/3[8]. H atoms were placed in idealized positions and refined using a riding model.

The crystal structures of **MoSiF3**, **MoSiF9** and **MoSi*F9-MCBD** suffer from disorder and the respective groups were refined with a disorder model where applicable. In case of **MoSi*F9-MCBD** the structure exhibits a fourfold modulation along the *c*-axis. For most of the ligands in this structure we were not able to refine a stable discrete disorder model. The structure of **MoSiF9-MCBD** was refined as an inversion twin with a minor component contribution of ca. 8 %. The crystal of **MoSiF9** decomposed during the measurement possibly because of a phase transition at 100K. Omission of the affected data led to a low completeness.

Molecular structures were pictured with the program *Ortep*[9]. Bond lengths and angles were determined using the programs *Diamond*[10] and *Mercury*[11].

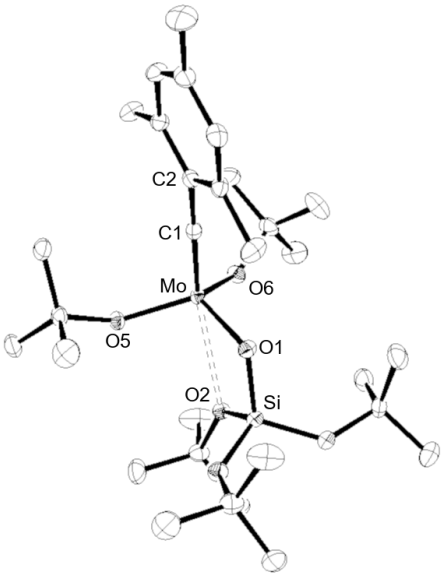


*Figure S37. Molecular structure of **MoSiF0** with thermal displacement parameters drawn at 50% probability; hydrogen atoms are omitted for clarity.*

*Table S5. crystallographic details of **MoSiF0**.*

| CCDC | **2074892** | |
|---|---|---|
| Empirical formula | $C_{30}H_{56}MoO_6Si$ | |
| Formula weight | 636.77 | |
| Temperature | 100(2) K | |
| Wavelength | 0.71073 Å | |
| Crystal system | monoclinic | |
| Space group | $P2_1/c$ | |
| Unit cell dimensions | a = 9.8096(2) Å | α= 90° |
| | b = 19.2702(5) Å | β= 94.181(3)° |
| | c = 18.5164(5) Å | γ= 90° |
| Volume | 3490.88(15) Å$^3$ | |
| Z | 4 | |
| Density (calculated) | 1.212 Mg/m$^3$ | |
| Absorption coefficient | 0.445 mm$^{-1}$ | |
| F(000) | 1360 | |
| Crystal size | 0.40 x 0.30 x 0.25 mm$^3$ | |
| Theta range for data collection | 2.335 to 31.052° | |
| Index ranges | −13≤h≤14, −27≤k≤27, −25≤l≤25 | |
| Reflections collected | 92385 | |
| Independent reflections | 10489 [R(int) = 0.0497] | |
| Completeness to theta = 30.00° | 98.7 % | |
| Absorption correction | Semi-empirical from equivalents | |
| Max. and min. transmission | 1.00000 and 0.98372 | |
| Refinement method | Full-matrix least-squares on $F^2$ | |
| Data / restraints / parameters | 10489 / 0 / 361 | |
| Goodness-of-fit on $F^2$ | 1.040 | |
| Final R indices [I>2sigma(I)] | R1 = 0.0294, wR2 = 0.0627 | |
| R indices (all data) | R1 = 0.0411, wR2 = 0.0673 | |
| Largest diff. peak and hole | 0.474 and -0.378 e.Å$^{-3}$ | |

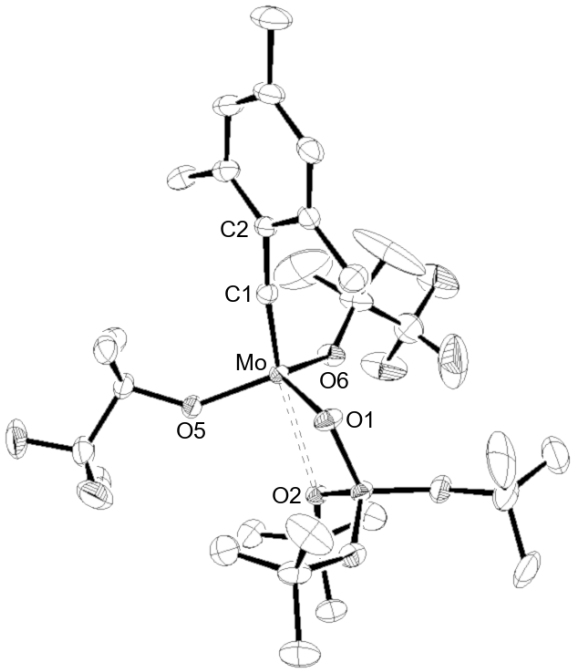


*Figure S38. Molecular structure of **MoSiF3** with thermal displacement parameters drawn at 50% probability; hydrogen atoms are omitted for clarity.*

*Table S6. crystallographic details of **MoSiF3**.*

| CCDC | **2074893** | |
|---|---|---|
| Empirical formula | $C_{30}H_{50}F_6MoO_6Si$ | |
| Formula weight | 744.73 | |
| Temperature | 100(2) K | |
| Wavelength | 0.71073 Å | |
| Crystal system | tetragonal | |
| Space group | $I4_1/a$ | |
| Unit cell dimensions | a = 35.4244(6) Å | α= 90° |
| | b = 35.4244(6) Å | β= 90° |
| | c = 11.8026(3) Å | γ= 90° |
| Volume | 14810.9(5) $Å^3$ | |
| Z | 16 | |
| Density (calculated) | 1.336 $mg/m^3$ | |
| Absorption coefficient | 0.453 $mm^{-1}$ | |
| F(000) | 6208 | |
| Crystal size | 0.35 x 0.35 x 0.25 $mm^3$ | |
| Theta range for data collection | 2.30 to 30.97° | |
| Index ranges | −51≤h≤47, −49≤k≤50, −16≤l≤17 | |
| Reflections collected | 116302 | |
| Independent reflections | 11197 [R(int) = 0.0502] | |
| Completeness to theta = 30.50° | 97.8 % | |
| Absorption correction | Semi-empirical from equivalents | |
| Max. and min. transmission | 1.00000 and 0.94363 | |
| Refinement method | Full-matrix least-squares on $F^2$ | |
| Data / restraints / parameters | 11197 / 195 / 487 | |
| Goodness-of-fit on $F^2$ | 1.040 | |
| Final R indices [I>2sigma(I)] | R1 = 0.0382, wR2 = 0.0808 | |

| | |
|---|---|
| R indices (all data) | R1 = 0.0554, wR2 = 0.0882 |
| Largest diff. peak and hole | 0.723 and -0.651 e.Å$^{-3}$ |

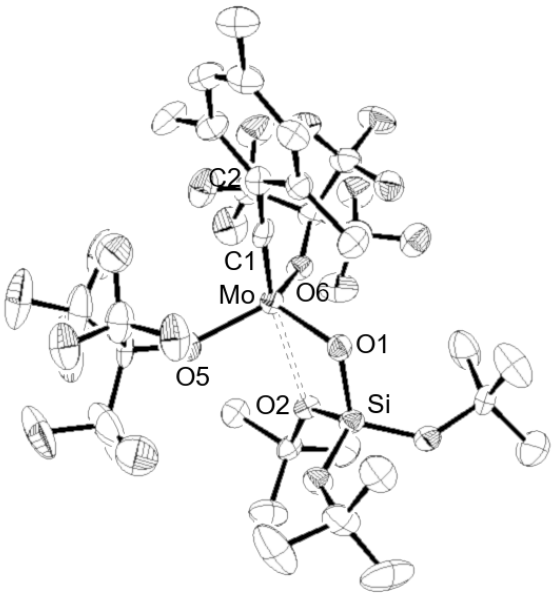


*Figure S39. Molecular structure of **MoSiF9** with thermal displacement parameters drawn at 50% probability; hydrogen atoms are omitted for clarity.*

*Table S7. crystallographic details of **MoSiF9**.*

| CCDC | **2074894** | |
|---|---|---|
| Empirical formula | $C_{30}H_{38}F_{18}MoO_6Si$ | |
| Formula weight | 960.63 | |
| Temperature | 100(2) K | |
| Wavelength | 1.54184 Å | |
| Crystal system | monoclinic | |
| Space group | $P2_1/c$ | |
| Unit cell dimensions | a = 16.9928(7) Å | α= 90° |
| | b = 18.5398(8) Å | β= 105.389(3)° |
| | c = 13.2555(5) Å | γ = 90° |
| Volume | 4026.3(3) Å$^3$ | |
| Z | 4 | |
| Density (calculated) | 1.585 mg/m$^3$ | |
| Absorption coefficient | 4.081 mm$^{-1}$ | |
| F(000) | 1936 | |
| Crystal habitus | irregular (orange) | |
| Crystal size | 0.320 x 0.170 x 0.140 mm$^3$ | |
| Theta range for data collection | 3.599 to 76.251° | |
| Index ranges | −19≤h≤19, −22≤k≤18, −11≤l≤14 | |
| Reflections collected | 16244 | |
| Independent reflections | 6056 [R(int) = 0.0597] | |
| Completeness to theta = 67.684° | 76.8 % | |
| Absorption correction | Gaussian | |
| Max. and min. transmission | 0.979 and 0.954 | |

| | |
|---|---|
| Refinement method | Full-matrix least-squares on $F^2$ |
| Data / restraints / parameters | 6056 / 0 / 517 |
| Goodness-of-fit on $F^2$ | 1.031 |
| Final R indices [I>2sigma(I)] | R1 = 0.0478, wR2 = 0.1226 |
| R indices (all data) | R1 = 0.0610, wR2 = 0.1334 |
| Largest diff. peak and hole | 0.983 and -0.897 e.Å$^{-3}$ |

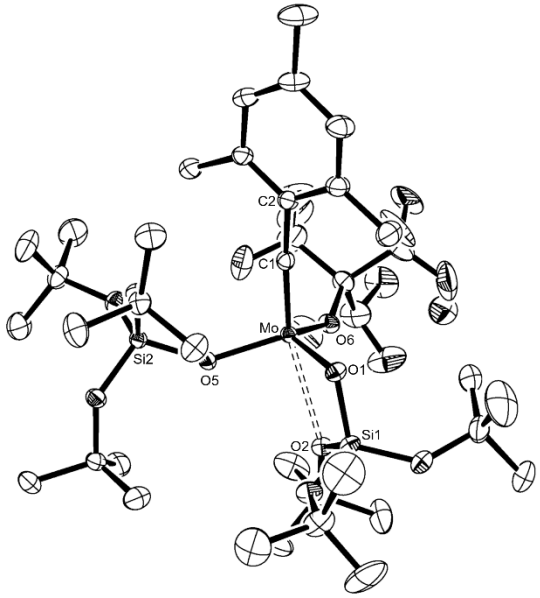


*Figure S40. Molecular structure of **MoSi2F9** with thermal displacement parameters drawn at 50% probability; hydrogen atoms are omitted for clarity.*

*Table S8. Crystallographic details of **MoSi2F9**.*

| CCDC | **2074895** |
|---|---|
| Empirical formula | $C_{38}H_{65}F_9MoO_9Si_2$ |
| Formula weight | 989.02 |
| Temperature | 130(2) K |
| Wavelength | 0.71073 Å |
| Crystal system | monoclinic |
| Space group | $P\,2_1/c$ |
| Unit cell dimensions | a = 11.5736(2) Å α= 90°<br>b = 21.7942(4) Å β= 100.760(2)°<br>c = 19.6903(5) Å γ = 90° |
| Volume | 4879.29(18) Å$^3$ |
| Z | 4 |
| Density (calculated) | 1.346 mg/m$^3$ |
| Absorption coefficient | 0.398 mm$^{-1}$ |
| F(000) | 2064 |
| Crystal habitus | irregular (orange) |
| Crystal size | 0.35 x 0.35 x 0.25 mm$^3$ |
| Theta range for data collection | 2.304 to 31.069° |
| Index ranges | −16≤h≤15, −31≤k≤31, −27≤l≤28 |
| Reflections collected | 128731 |
| Independent reflections | 14665 [R(int) = 0.0490] |
| Completeness to theta = 30.00° | 99.0 % |
| Absorption correction | Semi-empirical from equivalents |
| Max. and min. transmission | 1.00000 and 0.97935 |
| Refinement method | Full-matrix least-squares on $F^2$ |
| Data / restraints / parameters | 14665 / 348 / 602 |

| | |
|---|---|
| Goodness-of-fit on $F^2$ | 1.046 |
| Final R indices [I>2sigma(I)] | R1 = 0.0342, wR2 = 0.0724 |
| R indices (all data) | R1 = 0.0509, wR2 = 0.0800 |
| Largest diff. peak and hole | 0.538 and −0.436 e.$Å^{-3}$ |

*Table S9. Crystallographic details of **MoSi*F9**.*

| CCDC | **2074896** | |
|---|---|---|
| Empirical formula | $C_{35}H_{40}F_{18}MoO_6Si$ | |
| Formula weight | 1022.70 | |
| Temperature | 100(2) K | |
| Wavelength | 1.54184 Å | |
| Crystal system | monoclinic | |
| Space group | $P2_1/n$ | |
| Unit cell dimensions | a = 13.0531(2) Å | α= 90° |
| | b = 10.2588(2) Å | β= 95.337(2)° |
| | c = 32.3183(6) Å | γ = 90° |
| Volume | 4308.95(13) Å$^3$ | |
| Z | 4 | |
| Density (calculated) | 1.576 mg/m$^3$ | |
| Absorption coefficient | 3.855 mm$^{-1}$ | |
| F(000) | 2064 | |
| Crystal habitus | block (yellow) | |
| Crystal size | 0.121 x 0.056 x 0.047 mm$^3$ | |
| Theta range for data collection | 2.746 to 77.547° | |
| Index ranges | −16≤h≤16, −13≤k≤12, −40≤l≤31 | |
| Reflections collected | 70721 | |
| Independent reflections | 8988 [R(int) = 0.0401] | |
| Completeness to theta = 67.684° | 99.9 % | |
| Absorption correction | Gaussian | |
| Max. and min. transmission | 0.979 and 0.758 | |
| Refinement method | Full-matrix least-squares on F$^2$ | |
| Data / restraints / parameters | 8988 / 0 / 562 | |
| Goodness-of-fit on F$^2$ | 1.044 | |
| Final R indices [I>2sigma(I)] | R1 = 0.0363, wR2 = 0.0924 | |
| R indices (all data) | R1 = 0.0402, wR2 = 0.0946 | |
| Largest diff. peak and hole | 0.773 and -0.532 e.Å$^{-3}$ | |

Table S10. crystallographic details of **MoSiF9-MCBD**.

| CCDC | **2074896** | |
|---|---|---|
| Empirical formula | $C_{29}H_{42}F_{18}MoO_6Si$ | |
| Formula weight | 952.65 | |
| Temperature | 100(2) K | |
| Wavelength | 1.54184 Å | |
| Instrument (scan mode) | Oxford Diffraction Xcalibur, Atlas, Nova (ω scans) | |
| Crystal system | orthorhombic | |
| Space group | *Fdd2* | |
| Unit cell dimensions | a = 39.5833(4) Å | α= 90° |
| | b = 38.8824(4) Å | β= 90° |
| | c = 10.0284(2) Å | γ = 90° |
| Volume | 15434.6(4) Å$^3$ | |
| Z | 16 | |
| Density (calculated) | 1.640 mg/m$^3$ | |
| Absorption coefficient | 4.249 mm$^{-1}$ | |
| F(000) | 7712 | |
| Crystal habitus | irregular (violett) | |
| Crystal size | 0.147 x 0.100 x 0.086 mm$^3$ | |
| Theta range for data collection | 3.186 to 76.103° | |
| Index ranges | −49≤h≤49, −48≤k≤48, −12≤l≤12 | |
| Reflections collected | 142515 | |
| Independent reflections | 7889 [R(int) = 0.0692] | |
| Completeness to theta = 67.684° | 100 % | |
| Absorption correction | Gaussian | |
| Max. and min. transmission | 0.987 and 0.977 | |
| Refinement method | Full-matrix least-squares on F$^2$ | |
| Data / restraints / parameters | 7889 / 1 / 509 | |
| Goodness-of-fit on F$^2$ | 1.073 | |
| Final R indices [I>2sigma(I)] | R1 = 0.0365, wR2 = 0.0952 | |
| R indices (all data) | R1 = 0.0379, wR2 = 0.0964 | |
| Largest diff. peak and hole | 1.127 and -0.910 e.Å$^{-3}$ | |

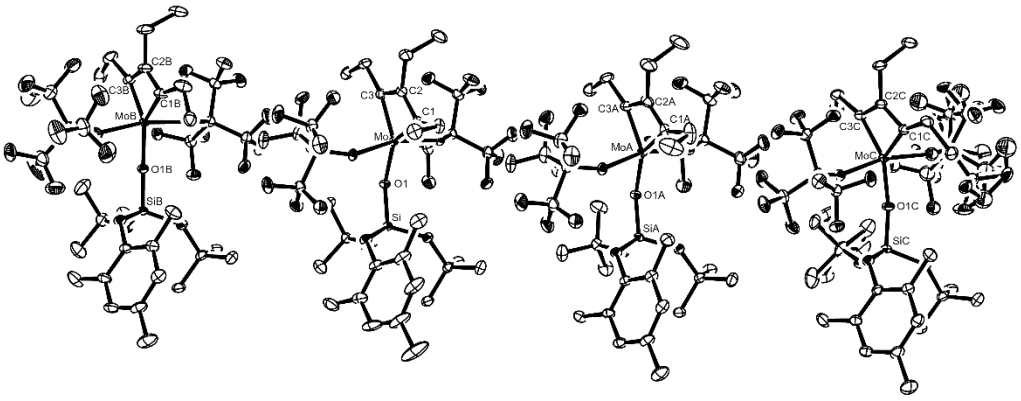


*Figure S41. crystal structure of the four independent molecules from **MoSi*F9-MCBD** with thermal displacement parameters drawn at 50% probability; hydrogen atoms are omitted for clarity.*

*Table S11. crystallographic details of **MoSi*F9-MCBD**.*

| CCDC | **2074898** | |
|---|---|---|
| Empirical formula | $C_{34}H_{44}F_{18}MoO_6Si$ | |
| Formula weight | 1014.72 | |
| Temperature | 100(2) K | |
| Wavelength | 0.71073 Å | |
| Crystal system | monoclinic | |
| Space group | $P2_1/n$ | |
| Unit cell dimensions | a = 22.4338(3) Å | α= 90° |
| | b = 19.5534(3) Å | β= 97.4393(12)° |
| | c = 38.0768(5) Å | γ = 90° |
| Volume | 16562.1(4) Å$^3$ | |
| Z | 16 | |
| Density (calculated) | 1.628 mg/m$^3$ | |
| Absorption coefficient | 0.469 mm$^{-1}$ | |
| F(000) | 8224 | |
| Crystal habitus | irregular (purple) | |
| Crystal size | 0.243 x 0.191 x 0.119 mm$^3$ | |
| Theta range for data collection | 1.682 to 36.319° | |
| Index ranges | −37≤h≤37, −32≤k≤32, −63≤l≤63 | |
| Reflections collected | 910394 | |
| Independent reflections | 80289 [R(int) = 0.0816] | |
| Completeness to theta = 25.242° | 100 % | |
| Absorption correction | Gaussian | |
| Max. and min. transmission | 1.000 and 0.474 | |
| Refinement method | Full-matrix least-squares on F$^2$ | |
| Data / restraints / parameters | 80289 / 0 / 2297 | |
| Goodness-of-fit on F$^2$ | 1.143 | |
| Final R indices [I>2sigma(I)] | R1 = 0.0697, wR2 = 0.1338 | |
| R indices (all data) | R1 = 0.0995, wR2 = 0.1441 | |
| Largest diff. peak and hole | 2.792 and −1.762 e.Å$^{-3}$ | |

## Alkyne Metathesis

**General Procedure for Homometathesis.** In a glove box, a 50 mL flask was charged with molecular sieve 5 Å (500 mg), *n*-decane (48.7 µL, 1 eq.) as internal standard and a solution of the substrate (0.5 mmol) in toluene (2.5 mL). Afterwards the precatalyst **MoSiF9** (1 mol%, 2.4 mg) or **MoSi*F9** (1 mol%, 2.6 mg) was added. Samples of 0.05 mL were taken at specific times (0, 1, 2, 3, 4, 5, 10, 20, 30, 60, 120, 240, 1440 min). The samples were filtered through a pad of silica and washed with diethyl ether (1.2 mL) before measuring it in gas chromatographic analysis.

**General Procedure for RCAM.** In a glove box, a 50 mL flask was charged with molecular sieve 5 Å (500 mg), *n*-decane (48.7 µL, 1 eq.) as internal standard and a solution of the substrate (0.25 mmol) in toluene (12 mL). Afterwards the precatalyst **MoSiF9** (2 mol%, 4.8 mg) or **MoSi*F9** (1 mol%, 2.6 mg) was added. Samples of 0.1 mL were taken at specific times (0, 1, 2, 3, 4, 5, 10, 20, 30, 60, 120(, 240, 1440)). The samples were filtered through a pad of silica and washed with diethyl ether (1 mL) before measuring it in gas chromatographic analysis.

**General Procedure for isolated Yields.** In a glove box, a 50 mL flask was charged with molecular sieve 5 Å (500 mg) and a solution of the substrate (0.5 mmol) in toluene (Homometathesis: 2.5 mL, RCAM: 12 mL). Afterwards the precatalyst **MoF9** (1 mol%, 4.7 mg), **MoSiF9** (Homometathesis: 1 mol%, 2.4 mg RCAM: 2 mol%, 4.8 mg) or **MoSi*F9** (1 mol%, 5.1 mg) was added. The solution was stirred for 2 h at rt. The pure products were obtained after filtration over silica, evaporation of the solvent in vacuo and a final column chromatography (*n*-hexane).

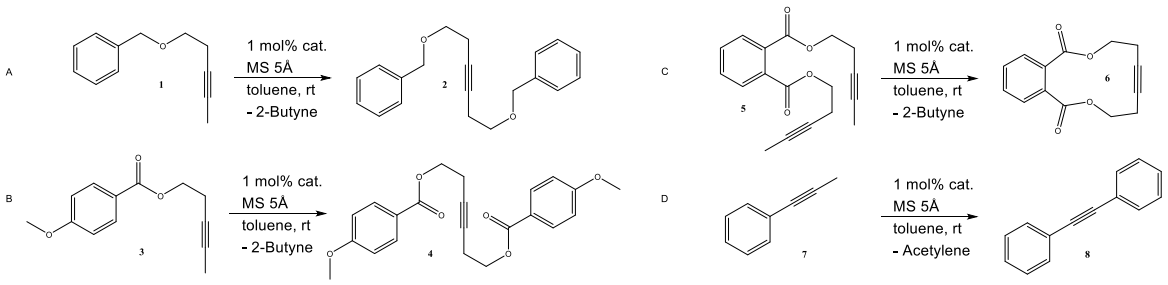


*Figure S42. Assignment of the alkyne metathesis reactions.*

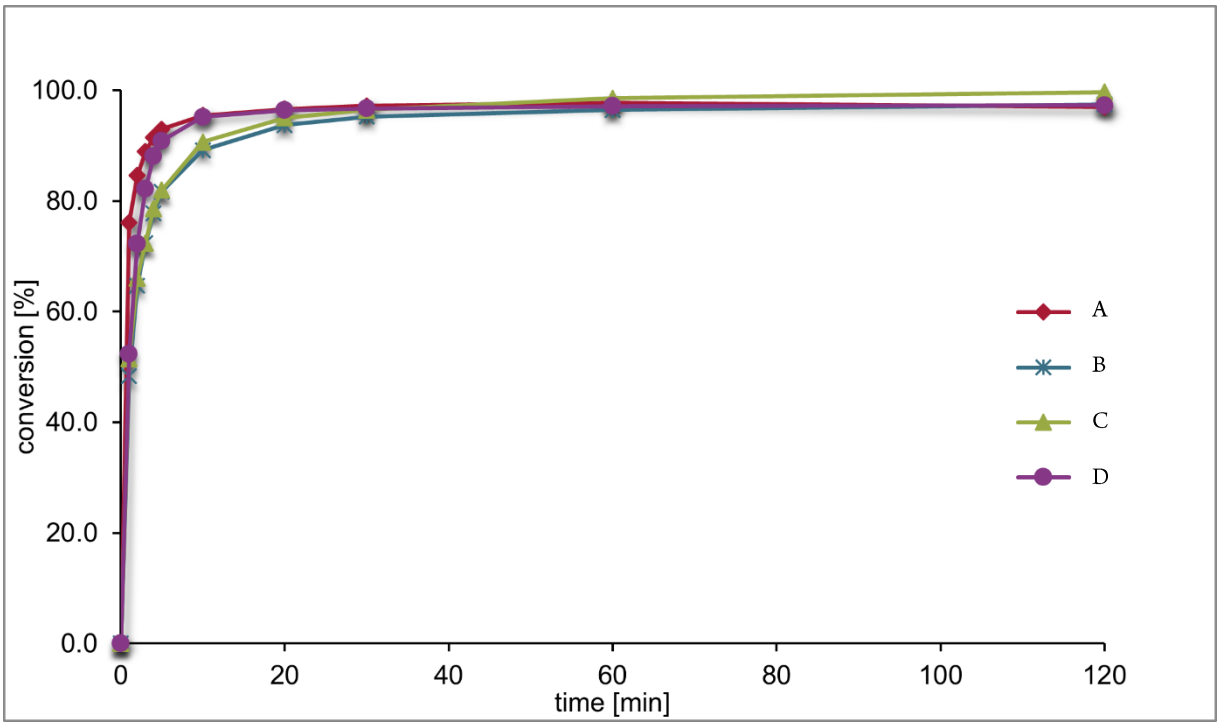


*Figure S43. Conversion-time plot of the metathesis with* ***MoSiF9****. GC-conversion after 2 h: A= 97%, B=97% , C= 99%, D= 97%.*

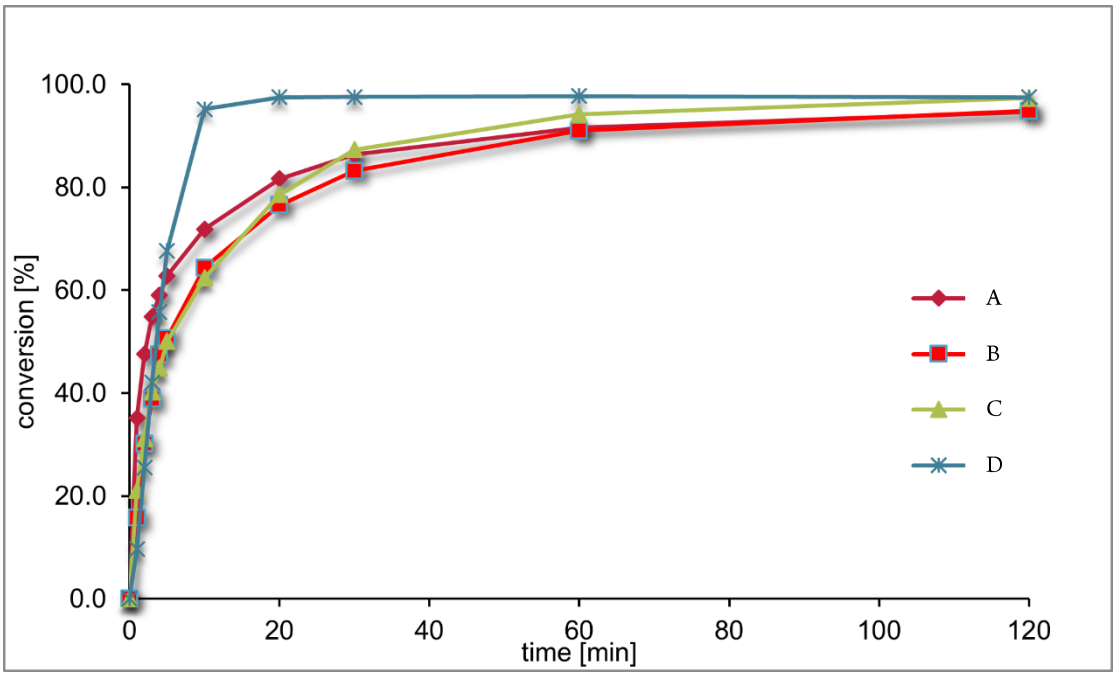


*Figure S44. Conversion-time plot of the metathesis with* ***MoSi*F9****. GC-conversion after 2 h: A= 95%, B=95% , C= 97%, D= 98%.*

**Synthesis of 1,6-bis(benzyloxy)hex-3-yne (2)**
The reaction took place according to the synthesis above with ((pent-3-yn-1-yloxy)methyl)benzene (91.4 mg, 0.52 mmol). Filtration over silica leaded the product as colorless liquid.

$Yield_{MoSiF9}$: 92% $Yield_{MoSi*F9}$: 97%.

**Synthesis of hex-3-yne-1,6-diyl bis(4-methoxybenzoate) (4)**
The reaction took place according to the synthesis above with pent-3-yn-1-yl 4-methoxybenzoate (112.7 mg, 0.51 mmol). Filtration over silica leaded the product as white solid.

$Yield_{MoSiF9}$: 99% $Yield_{MoSi*F9}$: 99%.

**Synthesis of 2,9-benzodioxacyclododecin-1,10-dione (6)**
The reaction took place according to the synthesis above with di(pent-3-yn-1-yl) phthalate (76.4 mg, 0.26 mmol). Filtration over silica leaded the product as white solid.

$Yield_{MoSiF9}$: 94% $Yield_{MoSi*F9}$: 95%.

**Synthesis of 1,2-diphenylacetylene (8)**
The reaction took place according to the synthesis above with prop-1-yn-1-ylbenzene (62,6 µL, 0.5 mmol). Filtration over silica leaded the product as white solid.
$Yield_{MoF9}$: 78% $Yield_{MoSiF9}$: 96% $Yield_{MoSi*F9}$: 88%.

## Diyne Disproportionation

**General Procedure for the catalyst examination via GC-experiments.** In a glove box, a 25 mL flask was charged with either no molecular sieve, MS 4 Å (250 mg), MS 5 Å (250 mg) or a mixture of MS 4 Å and 5 Å (each 125 mg), *n*-decane (1 eq.) as internal standard and diyne **9a** (0.25 mmol) in DCM or toluene (8 mL). Afterwards the precatalyst **MoF9** (2 mol%), **MoSiF9** (2mol%) or **MoSi*F9** (2 mol%) was added. Samples of 0.05 mL were taken at specific times (0, 1, 2, 3, 4, 5, 10, 20, 30, 60, 120, 240, 360, 480, 1440 min). The samples were filtered through a pad of silica and washed with diethyl ether (1.2 mL) before measuring it in gas chromatographic analysis. Results of these examinations are shown in Table S12.

*Table S12. GC-experiments at room temperature, 1 eq. n-decane as internal standard, 2 mol% catalyst-loading.*

| cat. | MS | solvent | GC-conv. [%] |
|---|---|---|---|
| **MoSi*F9** | - | DCM | 54 |
| | 5Å | DCM | 9 |
| | 4Å | DCM | 44 |
| | 4Å+5Å | DCM | 46 |
| | **4Å+5Å** | **toluene** | **92** |
| **MoSiF9** | - | DCM | 35 |
| | 5Å | DCM | 0 |
| | 4Å | DCM | 23 |
| | 4Å+5Å | DCM | 42 |
| | **4Å+5Å** | **toluene** | **86** |
| **MoF9** | - | DCM | 41 |
| | 5Å | DCM | 11 |
| | 4Å | DCM | 30 |
| | 4Å+5Å | DCM | 25 |
| | **4Å+5Å** | **toluene** | **89** |

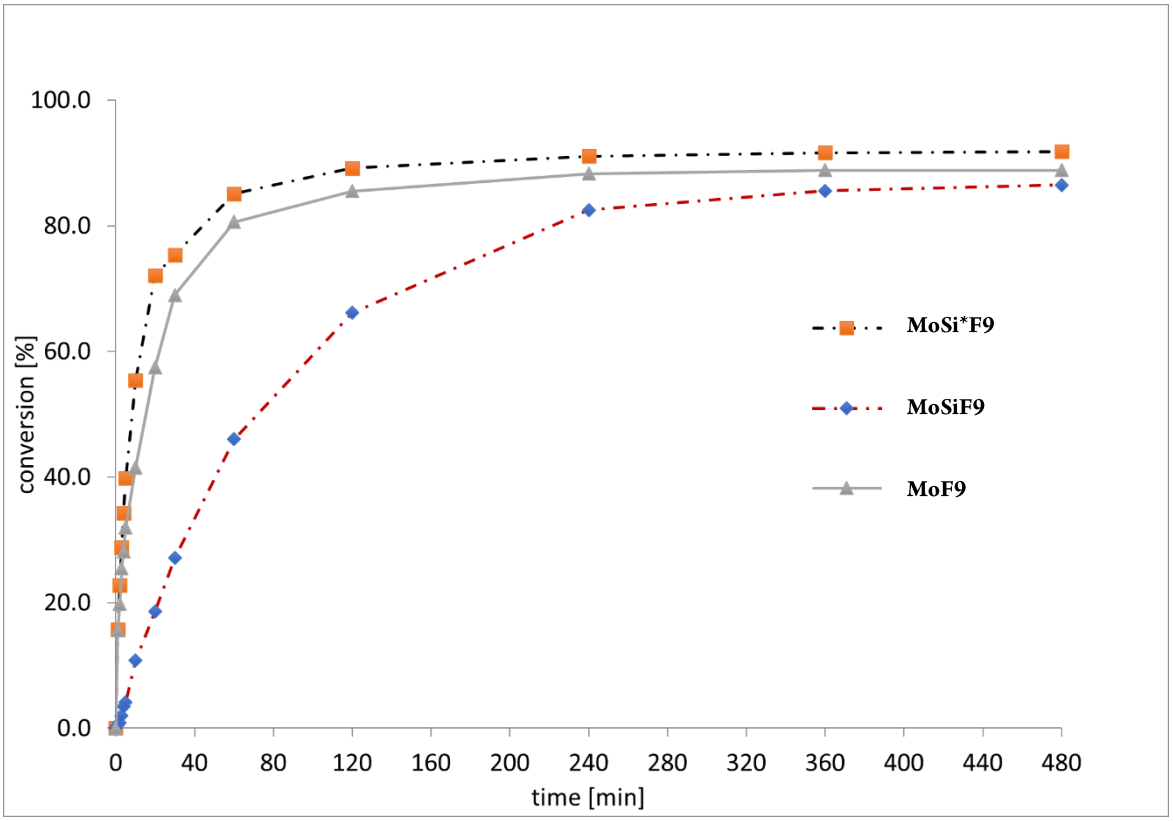


*Figure S45. Conversion-time plot of the diyne disproportionation of **9a** in toluene with MS 4 Å + 5 Å and 2 mol% catalyst loading. GC-conversion after 24h: **MoF9** 89%, **MoSiF9** 86%, **MoSi*F9** 92%.*

*Table S13. Isolated yields for the diyne disproportionation of the substrates **9a** and **9b**.*

| educt/product | **MoF9** | **MoSiF9** | **MoSi*F9** |
|---|---|---|---|
| **9a**/**10a**[c] | 82 | 79 | 88 |
| **9b**/**10b**[c] | 50 | 17 | 71 |

## Synthesis of TIPSC≡CC≡CC≡CTIPS (10a)

### ***MoF9***

In a glove box, a 25 mL flask was charged with toluene (2.5 mL) and diyne **9a** (115.1 mg, 0.52 mmol), before MS 4 Å (400 mg) and MS 5 Å (400 mg) were added. Afterwards, the precatalyst **MoF9** (1 mol%, 5.2 mg, 0.0053 mmol) was added. After stirring for four hours at rt, the reaction mixture was filtered through a pad of silica and rinsed with DCM and pentane. Evaporation of the solvent and recrystallization from MeOH yielded the product as white solid (82.8 mg, 0.21 mmol, 82 %). NMR spectroscopic data is in accordance with the literature.[12]

### ***MoSiF9***

In a glove box, a 25 mL flask was charged with toluene (2.5 mL) and diyne **9a** (109.3 mg, 0.5 mmol) before MS 4 Å (400 mg) and MS 5 Å (400 mg) were added. Afterwards, the precatalyst **MoSiF9** (1 mol%, 5.1 mg, 0.0053 mmol) was added. After stirring for four hours at rt, the reaction mixture was filtered through a pad of silica and rinsed with DCM and pentane. Evaporation of the solvent and

recrystallization from MeOH yielded the product as white solid (75.4 mg, 0.19 mmol, 79 %). NMR spectroscopic data is in accordance with the literature.[12]

***MoSi*F9***

In a glove box, a 25 mL flask was charged with toluene (2.5 mL) and diyne **9a** (117.0 mg, 0.53 mmol), before MS 4 Å (400 mg) and MS 5 Å (400 mg) were added. Afterwards, the precatalyst **MoSi*F9** (1 mol%, 6.0 mg, 0.0055 mmol) was added. After stirring for four hours at rt, the reaction mixture was filtered through a pad of silica and rinsed with DCM and pentane. Evaporation of the solvent and recrystallization from MeOH yielded the product as white solid (90.4 mg, 0.23 mmol, 88 %). NMR spectroscopic data is in accordance with the literature.[12]

**$^{1}$H NMR** (400 MHz, $CDCl_3$, 298 K): $\delta$ = 1.12–1.09 (m, 42H) ppm.

**$^{13}$C{$^{1}$H} NMR** (101 MHz, $CDCl_3$, 298K): $\delta$ = 89.9 (TIPSCCC), 84.9 (TIPSCCC), 61.5 (TIPSCCC), 18.7 ($CH_3$), 11.4 (CH) ppm.

**Synthesis of MesC≡CC≡CC≡CMes (10b)**

***MoF9***

In a glove box, a 25 mL flask was charged with toluene (2.5 mL) and diyne **9b** (93.4 mg, 0.5 mmol), before MS 4 Å (400 mg) and MS 5 Å (400 mg) were added. Afterwards, the precatalyst **MoF9** (1 mol%, 4.8 mg, 0.005 mmol) was added. After stirring for one hour at rt, the reaction mixture was filtered and rinsed with DCM and pentane. Evaporation of the solvent and recrystallization from MeOH yielded the product as white solid (38.5 mg, 0.12 mmol, 50 %).

***MoSiF9***

In a glove box, a 25 mL flask was charged with toluene (2.5 mL) and diyne **9b** (91.9 mg, 0.5 mmol), before MS 4 Å (400 mg) and MS 5 Å (400 mg) were added. Afterwards, the precatalyst **MoSiF9** (1 mol%, 4.9 mg, 0.005 mmol) was added. After stirring for one hour at rt, the reaction mixture was filtered and rinsed with DCM and pentane. Evaporation of the solvent and recrystallization from MeOH yielded the product as white solid (13.6 mg, 0.04 mmol, 17 %).

***MoSi*F9***

In a glove box, a 25 mL flask was charged with toluene (2.5 mL) and diyne **9b** (89 mg, 0.5 mmol), before MS 4 Å (400 mg) and MS 5 Å (400 mg) were added. Afterwards, the precatalyst **MoSi*F9** (1 mol%, 5.1 mg, 0.005 mmol) was added. After stirring for one hour at rt, the reaction mixture was filtered and rinsed with DCM and pentane. Evaporation of the solvent and recrystallization from MeOH yielded the product as white solid (53.6 mg, 0.17 mmol, 71 %).

**$^{1}$H NMR** (400 MHz, $CDCl_3$, 298 K): $\delta$ = 6.87 (s, 4H, $H_{Ar}$), 2.42 (s, 12H, *o*-$CH_3$), 2.29 (s, 6H, *p*-$CH_3$) ppm.

**$^{13}$C{$^{1}$H} NMR** (101 MHz, $CDCl_3$, 298K): $\delta$ = 142.7, 139.5, 128.0, 118.1, 81.5 (MesCCC), 77.2 (MesCCC), 67.8 (MesCCC), 21.6 (*p*-$CH_3$), 21.1 (*o*-$CH_3$) ppm.

**HRMS** (MALDI): calcd. for $C_{24}H_{22}$ $[M]^+$: 310.1716; found: 310.171.

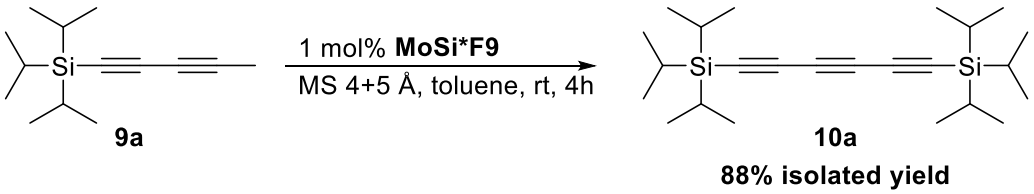


*Scheme S2. Diyne disproportionation of **9a**.*

**==== Shimadzu LabSolutions Analysis Report ====**

| | | | |
|---|---|---|---|
| Sample Name | : SR5-652 | | |
| Sample ID | : | | |
| Data Filename | : SR5-652.gcd | | |
| Method Filename | : GC1-TR5-80-340-M1.gcm | | |
| Batch Filename | : 1-[2020-07-07]-1.gcb | | |
| Vial # | : 2 | Sample Type | : Unknown |
| Injection Volume | : 1 uL | | |
| Date Acquired | : 07/07/2020 18:48:06 | Acquired by | : System Administrator |
| Date Processed | : 07/07/2020 19:15:22 | Processed by | : System Administrator |

**<Chromatogram>**

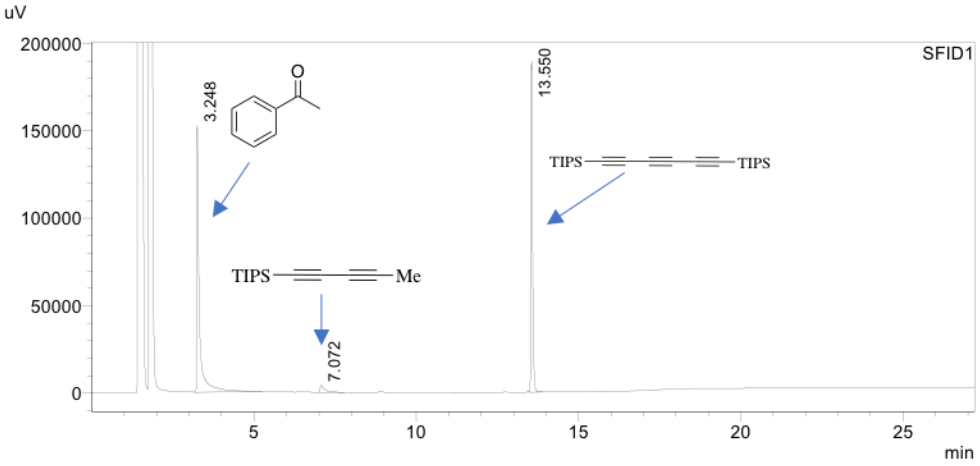


**<Peak Table>**

SFID1

| Peak# | Name | Ret. Time | Area | Height | Area% | Height% | Resolution(USP) |
|---|---|---|---|---|---|---|---|
| 1 | | 3.25 | 886111 | 151847 | 56.9 | 44.1 | -- |
| 2 | | 7.07 | 38023 | 3930 | 2.4 | 1.1 | 25.56 |
| 3 | | 13.55 | 633159 | 188811 | 40.7 | 54.8 | 46.35 |
| Total | | | 1557294 | 344587 | 100.0 | 100.0 | |

*Figure S46. Raw GC spectrum of the diyne disproportionation of **9a** shown in scheme S2.*

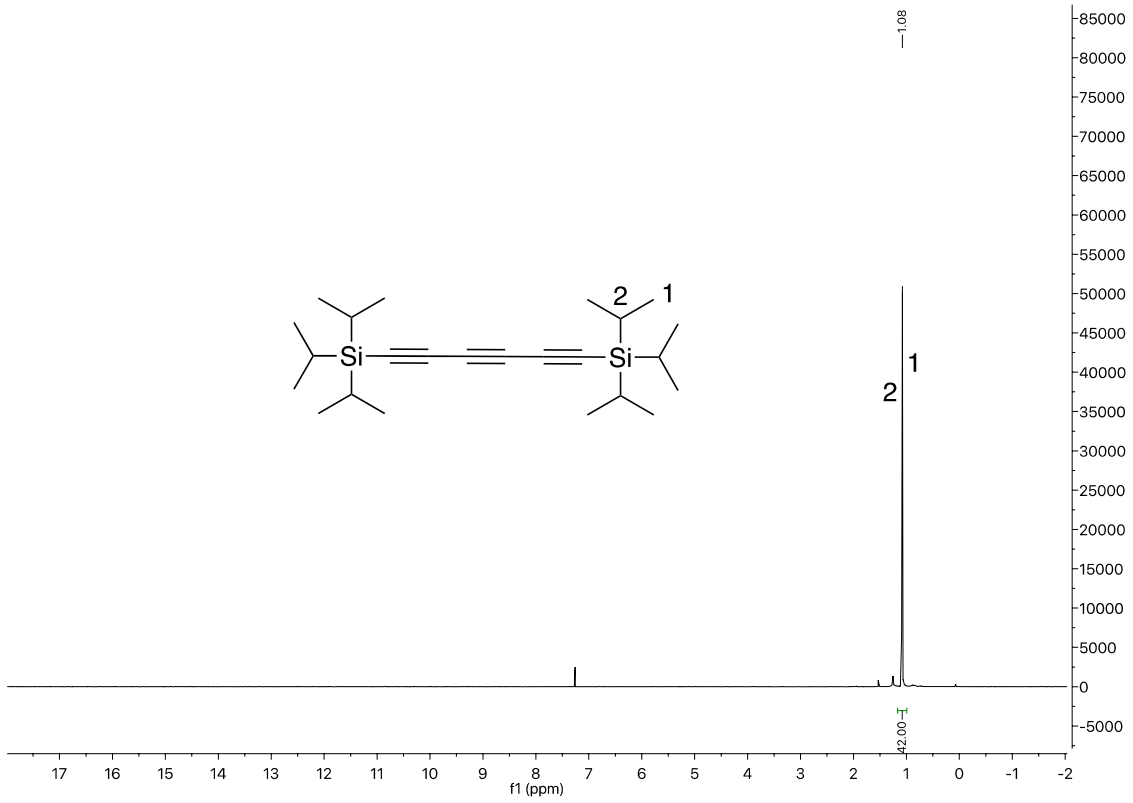


*Figure S47. $^{1}H$ NMR spectrum of **10a** in $CDCl_3$.*

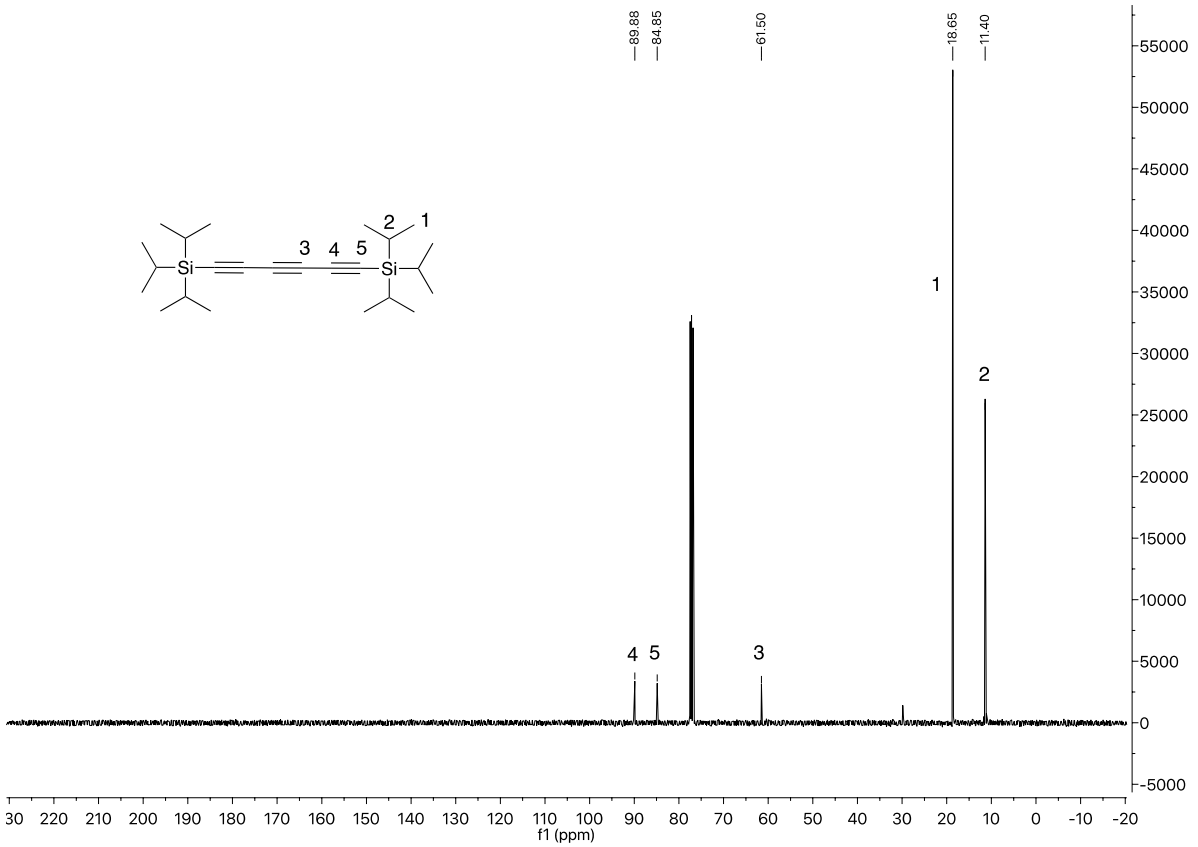


*Figure S48. $^{13}C\{^{1}H\}$ NMR spectrum of **10a** in $CDCl_3$.*


*Scheme S3. Diyne disproportionation of **9b**.*

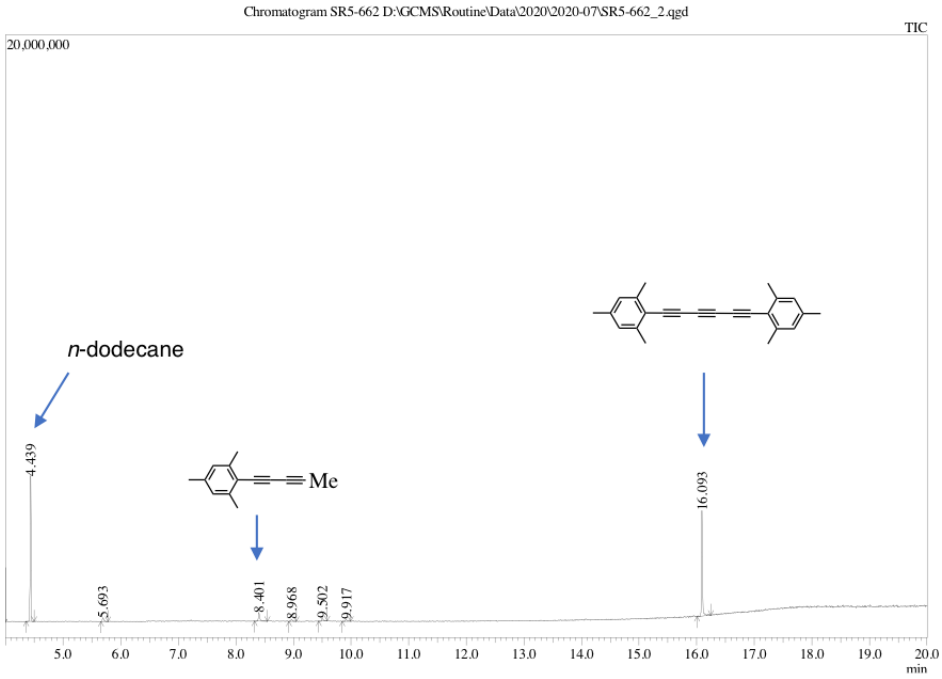


| Peak# | R.Time | Area | Area% | Height | Height% |
|---|---|---|---|---|---|
| 1 | 4.439 | 4805741 | 48.09 | 4956751 | 53.78 |
| 2 | 5.693 | 235519 | 2.36 | 132876 | 1.44 |
| 3 | 8.401 | 526981 | 5.27 | 297303 | 3.23 |
| 4 | 8.968 | 105305 | 1.05 | 65725 | 0.71 |
| 5 | 9.502 | 166580 | 1.67 | 117970 | 1.28 |
| 6 | 9.917 | 137832 | 1.38 | 58236 | 0.63 |
| 7 | 16.093 | 4015065 | 40.18 | 3587102 | 38.92 |
| | | 9993023 | 100.00 | 9215963 | 100.00 |

*Figure S49. Raw GC-MS spectrum of the diyne disproportionation of **9b** shown in scheme S3.*

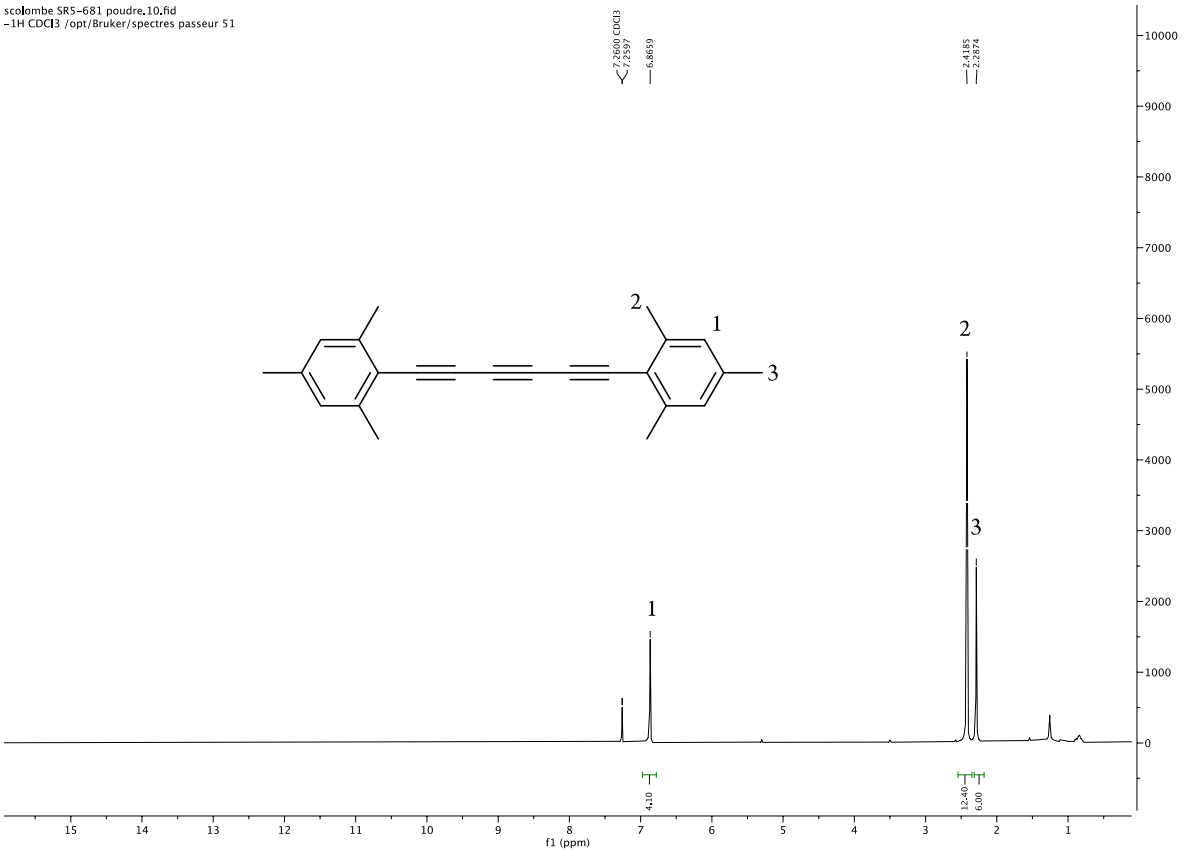


*Figure S50. $^{1}H$ NMR spectrum of **10b** in $CDCl_3$.*

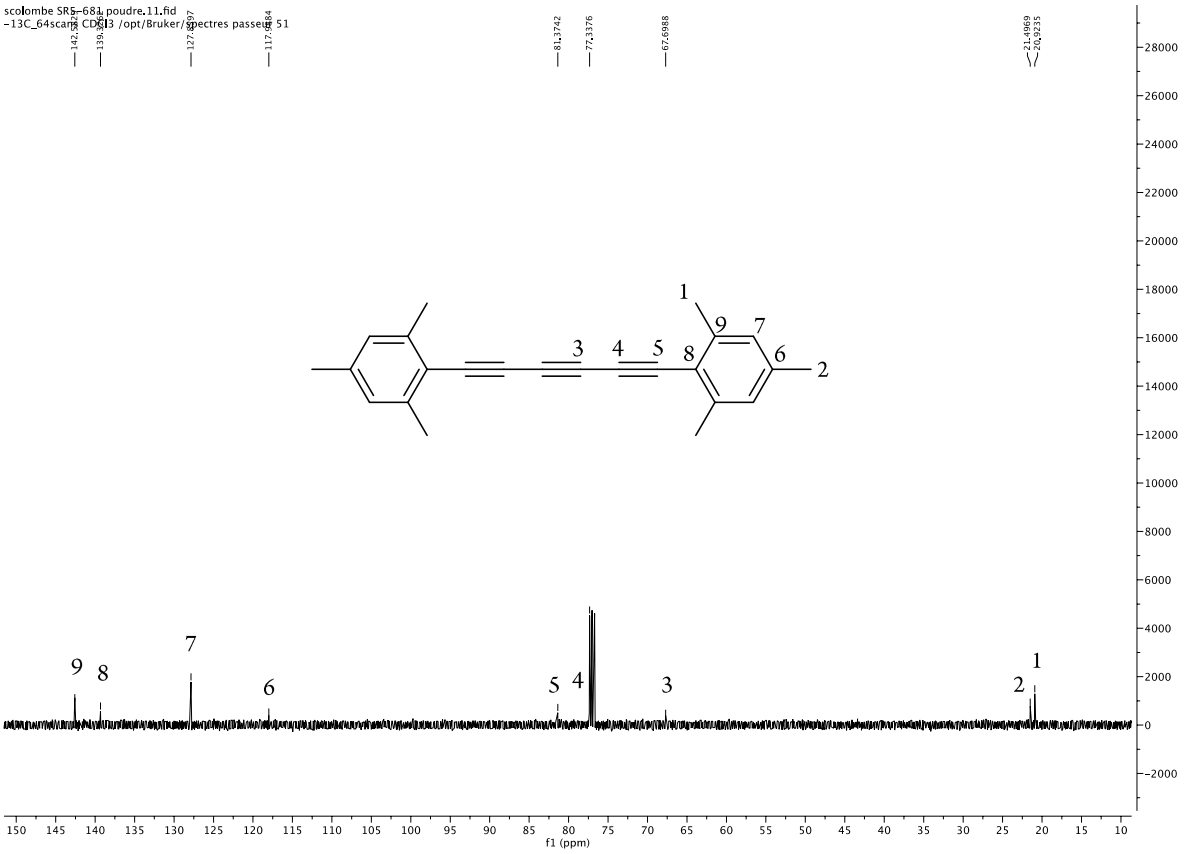


*Figure S51. $^{13}C\{^{1}H\}$ NMR spectrum of **10b** in $CDCl_3$.*

## References

(1) Haberlag, B.; Freytag, M.; Daniliuc, C. G.; Jones, P. G.; Tamm, M. Efficient metathesis of terminal alkynes. *Angew. Chem. Int. Ed. Engl.* **2012**, *51* (52), 13019–13022. DOI: 10.1002/anie.201207772.

(2) Bittner, C.; Ehrhorn, H.; Bockfeld, D.; Brandhorst, K.; Tamm, M. Tuning the Catalytic Alkyne Metathesis Activity of Molybdenum and Tungsten 2,4,6-Trimethylbenzylidyne Complexes with Fluoroalkoxide Ligands OC(CF 3 ) n Me 3– n (n = 0–3). *Organometallics* **2017**, *36* (17), 3398–3406. DOI: 10.1021/acs.organomet.7b00519.

(3) Lysenko, S.; Haberlag, B.; Daniliuc, C. G.; Jones, P. G.; Tamm, M. Efficient Catalytic Alkyne Metathesis with a Tri(tert-butoxy)silanolate-Supported Tungsten Benzylidyne Complex. *ChemCatChem* **2011**, *3* (1), 115–118. DOI: 10.1002/cctc.201000355.

(4) Docherty, S. R.; Estes, D. P.; Copéret, C. Facile Synthesis of Unsymmetrical Trialkoxysilanols: (RO) 2 (R′O)SiOH. *Helv. Chim. Acta* **2018**, *101* (3), e1700298. DOI: 10.1002/hlca.201700298.

(5) Rigaku Oxford Diffraction. *CrysAlisPRO Software System, versions 1.171.38.43 (2015), 1.171.40.61a (2019) and 1.171.40.81a (2020)*; Rigaku Corporation.

(6) Sheldrick, G. M. A short history of SHELX. *Acta Crystallogr., Sect. A: Found. Crystallogr.* **2008**, *64* (Pt 1), 112–122. DOI: 10.1107/S0108767307043930. Published Online: Dec. 21, 2007.

(7) Sheldrick, G. M. SHELXT - integrated space-group and crystal-structure determination. *Acta Crystallogr., Sect. A: Found. Adv.* **2015**, *71* (Pt 1), 3–8. DOI: 10.1107/S2053273314026370. Published Online: Jan. 1, 2015.

(8) Sheldrick, G. M. Crystal structure refinement with SHELXL. *Acta Crystallogr., Sect. C: Struct. Chem.* **2015**, *71* (Pt 1), 3–8. DOI: 10.1107/S2053229614024218. Published Online: Jan. 1, 2015.

(9) Farrugia, L. J. WinGX and ORTEP for Windows : an update. *J. Appl. Crystallogr.* **2012**, *45* (4), 849–854. DOI: 10.1107/S0021889812029111.

(10) K. Brandenburg. *Diamond*; Crystal Impact GbR.

(11) The Cambridge Crystallographic Data Centre. *Mercury CSD*; CCDC.

(12) Eisler, S.; Slepkov, A. D.; Elliott, E.; Luu, T.; McDonald, R.; Hegmann, F. A.; Tykwinski, R. R. Polyynes as a model for carbyne: synthesis, physical properties, and nonlinear optical response. *J. Am. Chem. Soc.* **2005**, *127* (8), 2666–2676. DOI: 10.1021/ja044526l.